

# Globular cluster formation with multiple stellar populations: self-enrichment in fractal massive molecular clouds

Kenji Bekki<sup>1\*</sup>

<sup>1</sup>*ICRAR M468 The University of Western Australia 35 Stirling Hwy, Crawley Western Australia 6009, Australia*

Accepted, Received 2005 February 20; in original form

## ABSTRACT

Internal chemical abundance spreads are one of fundamental properties of globular clusters (GCs) in the Galaxy. In order to understand the origin of such abundance spreads, we numerically investigate GC formation from massive molecular clouds (MCs) with fractal structures using our new hydrodynamical simulations with star formation and feedback effects of core-collapse supernovae (SNe) and asymptotic giant branch (AGB) stars. We particularly investigate star formation from gas chemically contaminated by SNe and AGB stars (‘self-enrichment’) in forming GCs within MCs with different initial conditions and environments. The principal results are as follows. GCs with multiple generation of stars can be formed from merging of hierarchical star cluster complexes that are developed from high-density regions of fractal MCs. Feedback effects of SNe and AGB stars can control the formation efficiencies of stars formed from original gas of MCs and from gas ejected from AGB stars. The simulated GCs have strong radial gradients of helium abundances within the central 3 pc. The original MC masses need to be as large as  $10^7 M_{\odot}$  for a canonical initial stellar mass function (IMF) so that the final masses of stars formed from AGB ejecta can be  $\sim 10^5 M_{\odot}$ . Since star formation from AGB ejecta is rather prolonged ( $\sim 10^8$  yr), their formation can be strongly suppressed by SNe of the stars themselves. This result implies that the so-called mass budget problem is much more severe than ever thought in the self-enrichment scenario of GC formation and thus that IMF for the second generation of stars should be ‘top-light’.

**Key words:** galaxies: star clusters: general – galaxies: stellar content – galaxies:ISM – globular cluster: general – stars:formation

## 1 INTRODUCTION

It has been established that internal chemical abundance spreads are one of fundamental properties of old globular clusters in the Galaxy (e.g., Gratton et al. 2012 for a recent review), the Large and Small Magellanic Clouds (e.g., Mucciarelli et al. 2009; Niederhofer et al. 2016), and the Galactic dwarf satellites (e.g., Carretta et al. 2010; Larsen et al. 2014). Most old GCs in the Galaxy show internal chemical abundance spreads in light elements (e.g., Carretta et al. 2009; C09) whereas only 8 of them have been so far observed to have internal [Fe/H] spreads (e.g., Marino et al. 2015). NGC 2808 and  $\omega$  Cen are GCs with He abundance spreads (e.g., Piotto et al. 2005), the origin of which remains unclear. The Galactic GC M22 is observed to have at least two groups of

stars with (i) the [Fe/H] difference of  $\sim 0.15$  dex among the two groups and (ii) higher abundance of *s*-process element in the Fe-rich group (e.g., Marino et al. 2009). The origin of the observed ubiquitous anti-correlations between light elements and different levels of internal abundance spreads in GCs are is one of unresolved problems in GC formation and evolution.

If these abundance spreads in various elements are due largely to secondary star formation from gas contaminated by earlier generation of stars within forming GCs (‘self-enrichment’), then we need to understand how such self-enrichment processes are possible in such compact stellar systems of GCs. Self-enrichment of pristine gas by AGB ejecta in forming GCs is demonstrated to be essentially important for the origin of the observed Na-O anticorrelations among GC stars (e.g., D’Ercole et al. 2010; D10). Self-enrichment processes by SNe could explain the observed

\* E-mail: kenji.bekki@uwa.edu.au

large metallicity spread and metallicity distribution function in  $\omega$  Cen (e.g., Ikuta & Arimoto 2000). Lee et al. (2009) found possible evidence of Ca abundance spreads in 7 Galactic GCs and thus suggested that self-enrichment processes by SNe are quite important for the origin of the observed spreads in  $[\text{Ca}/\text{Fe}]$ .

In spite of such importance of self-enrichment processes in GC formation, only several numerical simulations of GC formation have investigated the processes so far. Bekki & Chiba (2007) investigated how stellar wind of massive stars can influence the star formation processes and chemical evolution of forming GCs within turbulent, high-density giant MCs. They found that (i) second generation ('SG') of stars shows a C-N anticorrelation, (ii) the observed high  $[\text{N}/\text{Fe}]$  of  $\sim 0.8$  (e.g., NGC 6752) can not be reproduced in the simulated GCs for a canonical IMF, and (iii) the fraction of SG stars formed from gas contaminated by massive stars is quite small ( $\sim 3\%$ ). Using two-dimensional hydrodynamical simulations of star clusters (SCs) with stellar winds and SNe, Wünsch et al. (2008) performed 2D hydrodynamical simulations of young SCs with supernova winds and found that a significant fraction of SN ejecta can be still trapped in their inner regions if SCs are quite massive. Bekki (2010, 2011; B10 and B11, respectively) demonstrated that star formation from AGB ejecta can proceed very efficiently in clusters of first generation of stars ('FG'), as long as the clusters are massive enough ( $\geq 10^6 M_\odot$ ).

Although these previous simulations contributed to the better understanding of self-enrichment processes of GCs, the adopted initial conditions and models for GC formation are quite idealized and less realistic in the following points. First, these simulations do not consider the observed fractality of MCs (e.g., Blitz & Williams 1990; Bergin & Tafalla 2007). The fractal structures of MCs play key roles in the formation and evolution processes of SCs (e.g., Elmegreen 2008), and the observed ubiquitous SC complexes (e.g., Efremov 1995; Bastian et al. 2005; Adamo et al. 2012) can be developed from such fractal structures and thus important for GC formation (Bekki 2017; B17). Accordingly, the observed fractality needs to be included self-consistently in a more sophisticated simulation of GC formation. Second, feedback effects of SNe and AGB winds are not simultaneously and self-consistently included in previous simulations, which means that self-enrichment processes are not so realistic: either only chemical enrichment (and feedback effect) by SNe or only that by AGB stars was included in previous simulations. Accordingly, the previous models of GC formation did not predict possible abundance spreads in heavy elements (due to chemical enrichment by SNe) and in light elements (AGB stars).

Third, mass-dependent chemical yields of SNe and AGB are not properly included in previous chemodynamical simulations of GC formation. Given that chemical yields are different between SNe and AGB stars with different masses (e.g., Karakas 2010; K10) and star formation can proceed within a timescale of  $10^6$  yr, chemical abundance patterns of GC stars can depend strongly on which SNe or massive AGB stars can contribute to chemical enrichment processes within forming GCs. Accordingly time evolution of chemical abundances in ejecta of SNe and AGB stars needs to be included self-consistently. Fourth, secondary star formation from gaseous ejecta from SNe and AGB stars within

an existing single giant SC with the mass ( $M_{\text{sc}}$ ) larger than  $10^6 M_\odot$  is not so realistic, given that a SC is formed not in isolated but as a group of smaller clusters (e.g., Efremov 1995; Bastian et al. 2005). Therefore, self-enrichment processes investigated in previous 3D hydrodynamical simulations of GC formation (e.g., D'Ercole et al. 2008, D08; B10, B11) in a gravitational potential that is not evolving so much could be less realistic (B17). Thus, more realistic initial conditions of GC formation are required to be adopted so that self-enrichment processes of GCs can be better investigated in numerical simulations of GC formation.

The purpose of this paper is to investigate self-enrichment processes of GCs formed within massive MCs with fractal structures using new hydrodynamical simulations with feedback effects of SNe and AGB stars with different masses within MCs. We consider that GCs can be formed from massive MCs with masses larger than  $3 \times 10^6 M_\odot$  within gas-rich dwarf disk galaxies at high redshifts and thereby investigate the transformation from fractal MCs into compact stellar systems (GCs) in detail. We particularly investigate the following points: (i) how first generations of stars can be formed from cold gas of fractal MCs, (ii) whether new stars can be formed from gas ejected from SNe and AGB stars during merging of hierarchical star cluster complexes developed from fractal MCs, and (iii) how feedback effects of SNe and AGB winds influence the formation efficiencies of FG and SG stars in GCs. It should be noted here that AGB winds can significantly influence secondary star formation within forming GCs (Bekki 2016; B16).

The plan of the paper is as follows. We describe the models for massive MCs with fractal structures, feedback effects of SNe and AGB stars, chemical enrichment by these stars, star formation within MCs, and live gravitational potentials of GC-host dwarf galaxies in §2. We present the key results of the simulation, in particular, dynamics of GC formation from hierarchical star cluster complexes developed from fractal MCs and self-enrichment processes in GC formation in §3. Based on these results, we discuss (i) important roles of feedback effects of SNe and AGB stars in the physical properties of GCs and (ii) possibly different IMFs between FG and SG star formation in §4. We summarize our conclusions in §5. The physical meanings of acronym and symbols (e.g., FG and SG) often used in this paper are summarized in Table 1 for convenience.

In the present paper, we consider that the origin of the observed abundance spreads in the Galactic old GCs is due largely to multiple generations of stars in forming GCs. However, it is being hotly debated whether the observed extended main-sequence turn-offs (eMSTOs) and splits of main-sequence of the LMC clusters can result from age spreads (i.e., multiple generation of stars) or from internal stellar rotation (e.g., Bastian & De Mink 2009; Milone et al. 2016; Li et al. 2016). Accordingly, the above scenario of multiple generation of stars in the Galactic GCs could be just an assumption or hypothesis. However, For & Bekki (2017) have recently discovered young stellar objects (YSOs) with ages well less than  $10^6$  yr in the older LMC SCs with ages of 0.1–1 Gyr. This result is direct evidence for ongoing star formation in older LMC SCs and therefore strongly suggests that secondary star formation could have occurred in some of LMC SCs. Therefore, the above scenario of multiple generation of stars in forming GCs can be quite realistic, at least

**Table 1.** Description of (physical) meanings for acronym and symbols often used in the present study.

Acronym/Symbols	Physical meaning
SC	Star cluster
MC	Molecular cloud
SF	Star formation
FG	First generation of stars
SG	Second generation of stars
$D_3$	Fractal dimension (in 3D space) of a MC
$M_{\text{fg}}$	Total mass of FG stars
$M_{\text{sg}}$	Total mass of SG stars
$M_{\text{ns}}$	Total mass of new stars
$M_{\text{ej}}$	Gas mass ejected from SNe (AGB stars)
$\Sigma$	Surface mass density (e.g., $\Sigma_{\text{g}}$ for gas)
$\epsilon_{\text{sf,fg}}$	Star formation efficiency of FG stars
$\epsilon_{\text{sf,sg}}$	Star formation efficiency of SG stars
$t_{\text{agb}}$	Lifetime of stars that become AGB stars.
$t_{\text{delay,sg}}$	Time delay between SF and SNe in SG.
$\rho_{\text{th}}$	Threshold gas density for SF.

for some GCs, though the origin of the LMC SCs with multiple stellar populations can be different from that of GCs in galaxies other than the LMC.

## 2 THE MODEL

### 2.1 An overview

We consider that GCs can be formed from fractal MCs with their initial masses ( $M_{\text{mc}}$ ) much larger than the typical mass of the Galactic MCs in gas-rich dwarf galaxies at high redshifts. Harris & Pudritz (1994) proposed that GC-hosting MCs should be very massive (‘super-massive MCs’), because star formation efficiencies of MCs are typically rather low. The original mass of a MC ( $M_{\text{mc}}$ ) or a MC association (a group of giant MCs) hosting a GC with the initial mass of  $M_{\text{gc,i}}$  can be estimated from the final GC mass ( $M_{\text{gc,f}}$ ) by considering (i) star formation efficiency within the MC ( $\epsilon_{\text{sf}}$ ), (ii) gas ejection through SNe and AGB phases, and (ii) mass loss due to dynamical evolution (two-body relaxation and tidal stripping). The present-day (i.e., final) mass of the GC is as follows:

$$M_{\text{gc,f}} = (1 - f_{\text{strip}})(1 - f_{\text{ej}})M_{\text{gc,i}}, \quad (1)$$

where  $f_{\text{strip}}$  is the mass fraction of stars lost from the GC due to dynamical evolution and  $f_{\text{ej}}$  is the fraction of gas ejected from SNe and AGB stars. Therefore, the initial mass of GC-hosing cloud is simply as follows:

$$M_{\text{mc}} = \epsilon_{\text{sf}}^{-1} M_{\text{gc,i}}. \quad (2)$$

For a typical mass of the Galactic GCs ( $2 \times 10^5 M_{\odot}$ ), reasonable values of  $f_{\text{ej}} = 0.4$  and  $f_{\text{stri}} = 0.5$ , and rather high  $\epsilon_{\text{sf}} = 0.2$ ,  $M_{\text{mc}}$  can be therefore  $3.3 \times 10^6 M_{\odot}$ , which corresponds to the most massive GMCs in the Galaxy (e.g., Solomon et al. 1979). In this estimation, the initially rather large GC masses adopted in previous self-enrichment scenarios for multiple generation of stars in GCs (e.g., D08; B11) are not considered. If such GC masses are considered, then  $M_{\text{mc}}$  can be [5–10] times larger than the above value. Thus, we need to investigate GC formation in massive MCs with  $M_{\text{mc}} \geq 3 \times 10^6 M_{\odot}$  in order to discuss the physical properties of GCs.

Giant molecular clouds (GMCs) are observed to have fractal structures (e.g., Blitz et al. 2007), and their origin and nature have been extensively discussed both observationally and theoretically (e.g., Bergin & Tafalla 2007; Elmegreen 2008). However it is not so clear how such fractal structures can influence the formation processes of GCs, in particular, self-enrichment processes that lead to the formation of SG stars – the major component of GCs. The key parameter of fractal MCs is the fractal dimension ( $D_3$ ) in three-dimensional (3D) space. Recent observations have shown that  $D_3$  in interstellar medium, GMCs, and field stars are different depending on galaxy environments (e.g., Sun et al. 2016), which implies that we need to choose reasonable ranges of  $D_3$  depending on galaxy properties in the simulations of GC formation within MCs. By considering these observations, we investigate the influences of initial fractal structures of MCs on GC formation.

In order to perform smooth particle hydrodynamics (SPH) simulations of GC formation within massive MCs, we use our own original simulation code that can be run on GPU clusters (Bekki 2013, 2015). Although this code enables us to investigate the formation of molecular hydrogen ( $\text{H}_2$ ) from neutral one on dust grains, dust formation, destruction, and growth, effects of photo-electric heating on cold gas, star formation, SN feedback effects on star formation, we do not include dust-related physics in the present simulation. This is firstly because we do not focus on dust physics in GC formation in the present study, and secondly because simulations with such dust-related physics are very time-consuming (Bekki 2015). Since the details of the code are given in Bekki (2013, 2015), we briefly describe the code in the present study.

### 2.2 Massive molecular clouds

We adopt a size-mass relation that is consistent with (i) the observed relation between mass densities and sizes of GMCs discovered by Larson’s (1981) and (ii) the observed typical mass and size of GMCs in the Galaxy (e.g., Solomon et al. 1979). The following  $R_{\text{mc}} - M_{\text{mc}}$  relation is used for deriving the size of a massive MC ( $R_{\text{mc}}$ ) from the mass ( $M_{\text{mc}}$ ) for each MC;

$$R_{\text{mc}} = 40 \times \left( \frac{M_{\text{mc}}}{5 \times 10^5 M_{\odot}} \right)^{0.53} \text{pc} \quad (3)$$

We investigate models with  $M_{\text{mc}}$  ranging from  $3 \times 10^5 M_{\odot}$  to  $10^7 M_{\odot}$  in order to simulate massive SCs (GCs) with the initial total masses larger than  $10^5 M_{\odot}$ . This wide range of investigation can allow us to derive physical conditions for self-enrichment by AGB stars in a convincing manner.

A MC is assumed to have a power-law radial density profile ( $\rho_{\text{mc}}(r)$ ) as follows:

$$\rho_{\text{mc}}(r) = \frac{\rho_{\text{mc},0}}{(r + c_{\text{mc}})^{\beta}}, \quad (4)$$

where  $r$ ,  $\rho_{\text{mc},0}$ , and  $c_{\text{mc}}$ ,  $\beta$  are the distance from the MC’s center, a constant that is determined by  $M_{\text{mc}}$  and  $R_{\text{mc}}$ , the core radius of the MC, and the power-law slope. Although GMCs are observed to have  $\beta = 1 - 2$  (e.g., Ashman & Zepf 2001), we consider that  $\beta = 1$  is more reasonable. This is because the total mass of a GMC is roughly proportional to

$R^{3-\beta}$ , for which  $\beta = 1$  is consistent with the above mass-size relation ( $M_{\text{mc}} \propto R_{\text{mc}}^2$ ).

A MC is assumed to have a fractal gaseous distribution characterized by a fractal dimension  $D_3$ . The details of a way to set up the initial condition of a fractal structure for a given  $\beta$  are given in Appendix A. In the present model for fractal MCs, the power-law radial density profile of a MC can be seen even in the smallest substructure within the MC. Such a clumpy MC can show star formation in substructures from the earlier evolution of the MC so that low-mass unbound and bound SCs can be first formed from high-density regions of substructures. Therefore, dynamics of GC formation in fractal MCs can be significantly different from that in MCs without fractal structures. We consider that  $D_3 = 2$  is more consistent with  $\beta = 1$ , because  $M_{\text{mc}}$  is scaled to  $R_{\text{mc}}^{D_3}$  – a definition of fractal dimension. We therefore investigate the models with  $D_3 = 2$  more extensively, though we also investigate models with other  $\beta$  for comparison. The initial number of gas particles ( $N_g$ ) used in a simulation depends on  $D_3$  and  $N_{\text{min}}$ , which is the minimum number of gas particles used in the Level 1 distribution of gas particles (Appendix A). It is initially 1048911 for the fiducial model (described later) and the total gas particle number can increase with time owing to the ejection of gas from AGB stars.

The initial virial ratio ( $t_{\text{vir}}$ ) can determine the total amount of kinetic energy ( $T_{\text{kin}}$ ) of a MC and it is described as follows:

$$t_{\text{vir}} = \frac{2T_{\text{kin}}}{|W_{\text{mc}}|}, \quad (5)$$

where  $W_{\text{mc}}$  is the initial total potential energy of the MC. The random motion of each gas particle is determined by the above equation for a given spatial distribution of a MC. We investigate mainly the models with  $t_{\text{vir}} = 0.35$ , because the formation of compact stellar systems is ensured for that  $t_{\text{vir}}$  (e.g., Dale et al. 2014). We present only the results of the models with  $t_{\text{vir}} = 0.35$ , because other models with (i.e.,  $t_{\text{vir}} = 0.7$ ) show essentially similar behavior in GC formation. We also consider rigid rotation of a MC in some models, because previous observations suggested that velocity gradients within MCs could be due to such rotation (e.g., Phillips 1999; Rosolowsky et al. 2003). Since the magnitude of rigid rotation is not so well constrained, we assume that the amplitude of rigid rotation is a free parameter. Accordingly,  $T_{\text{kin}}$  is the combination of the total random energy  $T_{\text{ran}}$  and the total rotational one ( $T_{\text{rot}}$ ) as follows:

$$T_{\text{kin}} = T_{\text{ran}} + T_{\text{rot}}. \quad (6)$$

The way to give 3D velocities of gas particles based on  $T_{\text{ran}}$  and  $T_{\text{rot}}$  is given in Appendix.

In order to discuss the importance of initial rotation of MCs in GC formation, we introduce the following parameter:

$$f_{\text{rot}} = \frac{T_{\text{rot}}}{T_{\text{kin}}}. \quad (7)$$

We mainly discuss the results of the models with  $t_{\text{rot}} = 0$ , and we show the results for several rotating MC models with  $f_{\text{rot}} = 0.1$  in the present paper. Single massive stellar systems can be formed for such low  $f_{\text{rot}}$ . The results of models with larger  $f_{\text{rot}}$ , for which binary clusters can be formed, will be discussed in our forthcoming papers. Initial gaseous temperature and metallicity are set to be 10K and  $[\text{Fe}/\text{H}] = -2$  in all MCs. The radiative cooling processes are

**Table 2.** Description of key physical properties for the fiducial massive MC model.

Parameters	Values
Initial MC mass	$10^7 M_{\odot}$
Initial number of gas particles	1048911
Mass resolution	$9.5 \times 10 M_{\odot}$
Size resolution	0.39 pc
Number of AGB particles per a gas particle	5
Number of SNe types (in mass)	4
SN and AGB feedback from FG stars	Yes
SN and AGB feedback from SG stars	No
AGB yield	K10
SN yield	T95
Threshold gas density for star formation	$10^4 \text{ cm}^{-3}$
Tidal field from a dwarf host	No

properly included by using the cooling curve by Rosen & Bregman (1995) for  $T < 10^4 \text{K}$  and the MAPPING III code for  $T \geq 10^4 \text{K}$  (Sutherland & Dopita 1993).

### 2.3 Star formation and SN feedback

Gas particles can be converted into collisionless new stellar particles (‘new stars’) if the following two physical conditions can be met. First is that the local density ( $\rho_g$ ) exceeds a threshold density ( $\rho_{\text{th}}$ ) for star formation:

$$\rho_g > \rho_{\text{th}}. \quad (8)$$

We consider that star formation can proceed in the dense cores of MCs, and accordingly,  $\rho_{\text{th}}$  is set to be  $[10^4 - 10^5]$  H atoms  $\text{cm}^{-3}$ , which is consistent with the observed values (e.g., Bergin & Tafalla 2007). Second is that the local velocity field around a gas particle is consistent with that for gravitationally collapsing, which is formulated as follows

$$\text{div} \mathbf{v} < 0. \quad (9)$$

One SPH gas particle is converted into just one new star in the present study (i.e., not multiple times) so that the total particle number can not dramatically increase during a simulation.

Each new star particle is born with a fixed IMF and an initial mass  $m_{\text{ns}}$ : it should be noted here that this  $m_{\text{ns}}$  is not a mass of each individual star, which is denoted as  $m_s$ . The stellar mass decreases with time owing to mass loss by SNe Ia, SNe II, and, AGB stars and the final stellar mass after  $\sim 3 \times 10^8$  yr evolution (duration of a simulation) can be significantly different from  $m_{\text{ns}}$ . The mass loss from intermediate-mass and high-mass stars ( $m_s > 5 M_{\odot}$ ) plays a significant role in self-enrichment processes of GC formation in the present study. The adopted IMF in number is defined as  $\psi(m_s) = C_i m_s^{-\alpha}$ , where  $m_s$  is the initial mass of each individual star and the slope  $\alpha = 2.35$  corresponds to the Salpeter IMF. The normalization factor  $C_i$  is a function of a stellar particle mass,  $m_l$  (lower-mass cutoff), and  $m_u$  (upper-mass cutoff):

$$C_i = \frac{m_{\text{ns}} \times (2 - \alpha)}{m_u^{2-\alpha} - m_l^{2-\alpha}}. \quad (10)$$

where  $m_l$  and  $m_u$  are set to be  $0.1 M_{\odot}$  and  $120 M_{\odot}$ , respectively. Although we investigate only the models with  $\alpha = 2.35$  in the present study, the importance of top-heavy IMF in GC formation will be discussed in our forthcoming

papers based on the results of the models with lower  $\alpha$  (e.g.,  $\alpha = 1.85$ ).

SNe of new stars can give thermal and kinematic perturbation to their surrounding gas within GC-forming MCs. Each SN is assumed to eject the feedback energy ( $E_{\text{sn}}$ ) of  $10^{51}$  erg that is converted into thermal and kinetic energy of gas surrounding SN. Thornton et al. (1998) investigated how much fraction of  $E_{\text{sn}}$  of a SN can be used for the increase of random motion of the surrounding gas ('kinematic feedback'). In the present simulation, multiple SN explosion can occur within a single MC at different epochs within  $\sim 30$  Myr after star formation so that the energy-ratio of kinematic feedback to total SN energy ( $f_{\text{kin}}$ ) can be quite different from those predicted in previous simulations for single SN. We consider that  $f_{\text{kin}}$  is rather high owing to interaction of expanding shells formed from different SNe.

The way to distribute  $f_{\text{kin}}E_{\text{sn}}$  (i.e., kinetic feedback energy) of SNe among neighbor gas particles is described as follows. Each SN can eject gas with an initial ejection speed of  $v_{\text{ej}}$ , which is estimated from the following equation:

$$f_{\text{kin}}E_{\text{sn}} = 0.5(m_s - m_{\text{BH}})v_{\text{ej}}^2, \quad (11)$$

where  $m_{\text{BH}}$  is the mass of a black hole that is left after SN explosion for massive stars. The total mass of ejecta from a SN ( $m_{\text{ej}}$ ) depends on  $m_s$  owing to different  $m_{\text{BH}}$ . For  $m_s = 8M_{\odot}$  and  $f_{\text{kin}} = 1$ ,  $v_{\text{ej}} = 3800 \text{ km s}^{-1}$  ( $m_{\text{ej}} = 6.5M_{\odot}$ ). The kinetic energy of a SN is distributed equally among gas particles surrounding the SN. If there are  $N_{\text{nei}}$  gas particles around a SN, then  $j$ th gas particle can receive momentum of  $m_{\text{ej}}v_{\text{ej}}/N_{\text{nei}}$  so that its velocity can be changed as follows:

$$(m_j + m_{\text{ej}})v'_{j,k} = m_j v_{j,k} + m_{\text{ej}}v_{\text{ej}}, \quad (12)$$

where  $m_j$  is the mass of the gas particle before interaction with the SN,  $v_{j,k}$  and  $v'_{j,k}$  are the 3D velocity ( $k = 1, 2, 3$  correspond to  $x, y$ , and  $z$  components of the velocity) before and after gas-SN interaction, respectively. Although different SNe with different initial  $m_s$  explode at different times, we consider that one star formation event is followed by the following four SN events for different stellar mass ranges:  $m_s = [8 - 15]M_{\odot}$ ,  $m_s = [15 - 30]M_{\odot}$ ,  $m_s = [30 - 60]M_{\odot}$ , and  $m_s = [60 - 120]M_{\odot}$ . We adopt this model, because it is very time-consuming for the present study to change the 3D velocities (and chemical abundances) of gas particles around all SNe with different masses.

We consider that the time delay between conversion of gas into a new star and a SN explosion is parameterized by  $t_{\text{delay}}$ , which is describe as follows:

$$t_{\text{delay}} = t_{\text{to}} + t_{\text{sf}}, \quad (13)$$

where  $t_{\text{to}}$  is the main-sequence turn-off timescale and  $t_{\text{sf}}$  is the timescale of a pre-main sequence phase. Since the present simulation can not resolve the formation of individual stars from collapsing MC cores, we can not directly derive the timescale of a pre-main sequence phase. Given that the observed age of young stellar objects (YSOs) is  $\sim 10^6$  yr for massive stars (e.g., Whitney et al. 2008),  $t_{\text{sf}}$  could be at least  $10^6$  Myr. This  $t_{\text{sf}}$  is negligibly short in comparison with the main-sequence timescales of stars. We therefore investigated only the models with  $t_{\text{sf}} = 0$  in the present study. It should be noted here that  $t_{\text{sf}}$  can be quite long for low-mass stars. However, inclusion of such long  $t_{\text{sf}}$  for low-mass stars

in the present simulations would not change the present results significantly, because energetic feedback effects from low-mass stars on interstellar medium (ISM) are not possible.

In order to calculate  $t_{\text{to}}$  from the main-sequence turn-off mass ( $m_{\text{to}}$ ), we use the following formula (Greggio & Renzini 2011):

$$\log m_{\text{to}}(t_s) = 0.0434(\log t_s)^2 - 1.146 \log t_s + 7.119, \quad (14)$$

where  $m_{\text{to}}$  is in solar units and time  $t_s$  in years. Using the above equation, we can derive  $t_{\text{to}}$  for a given  $m_{\text{to}}$  ( $= m_s$ ). This is not a good approximation only for massive stars ( $m_s > 10M_{\odot}$  that explode as SNe; Greggio & Renzini 2011). For such massive stars, we adopt  $m_s = 3.0 \times 10^7$  yr,  $1.0 \times 10^7$  yr,  $4.9 \times 10^6$  yr, and  $3.4 \times 10^6$  yr for SNe with  $m_s = [8 - 15]M_{\odot}$ ,  $m_s = [15 - 30]M_{\odot}$ ,  $m_s = [30 - 60]M_{\odot}$ , and  $m_s = [60 - 120]M_{\odot}$ , respectively. The average SN explosion time ( $t_{\text{sn}}$ ) of these four discrete SN groups for the Salpeter IMF is  $1.42 \times 10^7$  yr.

Although time delay between star formation and SN explosion ( $t_{\text{delay,fg}}$ ) is considered to be dependent on  $m_s$  for all FG stars, we adopt a different model for time delay between star formation of SG stars and SN explosion ( $t_{\text{delay,sg}}$ ). This is because SG stars can be formed from AGB ejecta very efficiently in B10 and B11 in which SNe were not included at all (i.e., no SN feedback effects). We investigate how the SN explosion from SG stars can influence the formation processes of GCs with models with different  $t_{\text{delay,sg}}$ . If the upper-mass cutoff of the IMF ( $m_{\text{u}}$ ) is lower, then  $t_{\text{delay,sg}}$  can be longer. By changing  $t_{\text{delay,sg}}$ , we can discuss how the IMF of SG stars can control the physical properties of SG stars, which are the main components of GCs. We investigate the models without SNe from SG stars and those with  $t_{\text{delay,dg}} = 3$  Myr, 10 Myr, and 30 Myr.

## 2.4 Gas ejection and feedback effects from AGB stars

Since AGB stars can eject gas significantly later than SNe, SN explosion can expel almost all of original cold gas around intermediate-mass stars. Accordingly, there can be almost no gas around the stars when they start to eject gas during AGB phases. This is a serious problem in implementing chemical enrichment of gas by AGB ejecta if we adopt a standard model of chemical enrichment in which chemical abundances of gas particles can change only when the particles are within a certain radius from an AGB star: if no gas particles around an AGB star, the AGB ejecta can not be given to any particles (no chemical enrichment). This unrealistic situation needs to be avoided in the present simulation in which chemical enrichment processes are investigated. We therefore adopt a novel model (B16) in which each AGB star eject gas particles with chemical abundances predicted from recent AGB models (e.g., K10). Ejection of new particles from AGB stars ('AGB particle') means that the total number of gas particles can significantly increase as a simulation goes.

Chemical abundances of light elements are quite different between AGB stars with different masses (e.g., K10; Ventura et al. 2013), which means that SG stars formed from AGB ejecta at different times can have different abundances of light elements. In order to model chemical enrichment by

**Table 3.** The basic model parameters for fractal molecular clouds (MCs).

Model ID	$M_{\text{mc}}^a$	$R_{\text{mc}}^b$	$f_{\text{rot}}^c$	$D_3^d$	$t_{\text{delay,sn}}^e$	$r_p^f$	comments
M1	10	200	0	2	-	-	fiducial
M2	10	200	0	2	3	-	
M3	10	200	0	2	10	-	
M4	10	200	0	2	30	-	
M5	10	200	0	2	30	-	no SN feedback for FG an SG
M6	10	200	0.1	2	-	-	rotating MC
M7	10	200	0	2.4	-	-	larger fractal dimension
M8	10	200	0	2.4	3	-	
M9	10	200	0	3	-	-	large fractal dimension
M10	10	200	0	2	-	-	$\rho_{\text{th}} = 10^5 \text{ cm}^{-3}$
M11	10	200	0	2	3	-	$\rho_{\text{th}} = 10^5 \text{ cm}^{-3}$
M12	10	200	0	2	-	-	$\rho_{\text{mc}}(r) \propto r^{-2}$
M13	10	200	0	2	3	-	$\rho_{\text{mc}}(r) \propto r^{-2}$
M14	10	290	0	2	-	-	lower gas density
M15	10	139	0	2	-	-	higher gas density
M16	10	139	0	2	3	-	
M17	10	200	0	2	-	0.3	tidal field of MC-host galaxy
M18	10	200	0	2	-	1.0	
M19	3	100	0	2	-	-	
M20	3	100	0	2	3	-	
M21	3	100	0.1	2	-	-	
M22	3	100	0.1	2	3	-	
M23	3	100	0	2.4	-	-	
M24	3	100	0	2.4	3	-	
M25	3	69	0	2	-	-	
M26	3	69	0	2	3	-	
M27	3	100	0	2	-	-	$\rho_{\text{th}} = 10^5 \text{ cm}^{-3}$
M28	3	100	0	2	3	-	$\rho_{\text{th}} = 10^5 \text{ cm}^{-3}$
M29	3	100	0	2	-	0.3	
M30	3	100	0	2	-	1.0	
M31	1	68	0	2	-	-	
M32	1	68	0	2	3	-	
M33	1	68	0	2	-	-	$\rho_{\text{th}} = 10^5 \text{ cm}^{-3}$
M34	1	68	0	2.4	-	-	
M35	1	68	0	2.4	3	-	
M36	0.3	32	0	2	-	-	
M37	0.3	32	0	2	3	-	
M38	0.3	32	0	2	-	-	$\rho_{\text{th}} = 10^5 \text{ cm}^{-3}$

<sup>a</sup> The initial total mass of a fractal molecular cloud (MC) in units of  $10^6 M_{\odot}$ .

<sup>b</sup> The initial size for a MC in units of pc.

<sup>c</sup> The initial ratio of total rotational energy to total kinetic energy in a MC.

<sup>d</sup> The 3D fractal dimension of a MC.

<sup>e</sup> The time delay between star formation and the explosion of SNe in the formation of SG stars (Myr). The symbol ‘-’ means that no SNe can originate from SG stars owing to a top-light IMF in the model.

<sup>f</sup> The initial position of a MC with respect to the center of its host galaxy in unit of kpc. The symbol ‘-’ means that the model does not include the live gravitational potential of the MC-host galaxy.

AGB stars with different masses more properly, we consider ejection of AGB particles at different five epochs ( $t_{\text{agb}}$ , which corresponds to  $t_{\text{delay}}$  for intermediate-mass stars). These five are 200, 120, 80, 60, and 40 Myr and correspond to the lifetimes of the masses of stars, (i)  $3 \leq m_s < 4 (M_{\odot})$ , (ii)  $4 \leq m_s < 5 (M_{\odot})$ , (iii)  $5 \leq m_s < 6 (M_{\odot})$ , (iv)  $6 \leq m_s < 7 (M_{\odot})$ , and (v)  $7 \leq m_s < 8 (M_{\odot})$ , respectively. Here we consider only five different AGB particles, because we can not use excessively large number of gas particles owing to the limited amount of simulation time allocated to the project of the present study. The minimum mass of AGB stars ( $3M_{\odot}$ ) is chosen, firstly because age differences between FG and SG stars can not be too large, and secondary because the

fraction of gaseous ejecta from AGB stars with  $m_s < 3M_{\odot}$  is small.

An AGB particle is ejected from a new stellar particle with a wind velocity of  $v_{\text{wind}}$  at the end of the main-sequence phase of the stellar particle. Although this  $v_{\text{wind}}$  is an order of  $10 \text{ km s}^{-1}$ , such stellar wind can dramatically influence the star formation histories within existing SCs (e.g., D08, B10, B11, and B16): such stellar wind can be equivalent to kinematic feedback effects of SNe. We adopt  $v_{\text{wind}} = 10 \text{ km s}^{-1}$ , which is consistent with recent observations of AGB stars in the LMC (e.g., Marshall et al. 2004). The initial temperature of AGB wind ( $T_{\text{wind}}$ ) is set to be 1000 K, which is consistent with standard theoretical models of AGB winds. It is likely that SG formation from gas is possible only if

stellar wind can be efficiently cooled down from  $T_{\text{wind}}$  to a few tens K.

If the wind velocities of AGB stars in a proto-GC exceed the escape velocity ( $v_{\text{esc}}$ ) of the proto-GC, then the AGB ejecta is likely to escape from the proto-GC. This condition is simply described as follows:

$$v_{\text{wind}} > v_{\text{esc}} = f(M_{\text{mc}}, R_{\text{mc}}, D_3), \quad (15)$$

where  $v_{\text{esc}}$  is a function of  $M_{\text{mc}}$ ,  $R_{\text{mc}}$ , and  $D_3$ , all of which can determine the gravitational potential of the FG stellar systems. As shown in B11, low-mass FG systems are unlikely to retain AGB ejecta, because the above condition is not satisfied. Also, in order to understand the importance of AGB feedback effects on SG star formation, we investigated models with  $v_{\text{wind}} = 0$  and those with  $T_{\text{wind}} = 10$  K for comparison. We confirmed that both  $M_{\text{sg}}$  and  $\epsilon_{\text{sf,sg}}$  are higher in those models without AGB feedback effects, which is consistent with the results in B11 and B16. Since this result appears to be obvious (initially expected), we do not discuss these in this paper.

## 2.5 Chemical enrichment

Gaseous ejecta from a SN can mix with its surrounding gas particles so that the gas particles can increase their chemical abundances. We consider that such increment can occur if the gas particles are located within  $r_{\text{sn}}$  from the SN. This  $r_{\text{sn}}$  is set to be the initial gravitational softening length (0.4 pc). The chemical abundance of  $k$ th element ( $k=1, 2, 3, \dots$  correspond to H, He, C, N, O. ... respectively) for  $j$ th gas particle ( $Z_{j,k}$ ) among  $N_{\text{sn}}$  surrounding gas particles around a SN can change according to the following equation:

$$(m_j + m_{\text{ej}})Z'_{j,k} = m_j Z_{j,k} + \frac{\Delta m_{\text{ej}} Z_{\text{sn},k}}{N_{\text{sn}}}, \quad (16)$$

where  $Z'_{j,k}$  are the chemical abundance of  $k$ th element after chemical enrichment by the SN and  $Z_{\text{sn},k}$  is the chemical abundance of  $k$ th element for the SN ejecta. We use the chemical yield table of SNII from Tsujimoto et al. (1995, T95) to calculate  $Z_{\text{sn},k}$  in the present study. Since we will describe the chemical abundances of GC stars with different ages and locations within GCs and their dependencies on model parameters in our next paper, we briefly show some of the result in the present paper.

## 2.6 Live galactic potential

The tidal field of a dwarf galaxy hosting MCs can influence the formation processes of GCs within MCs during the orbital evolution of MCs around the MC-host dwarf. We therefore investigate such tidal effects on GC formation by constructing a model for live galactic potential of a dwarf galaxy as follows. We assume that a MC-host dwarf galaxy consists of a dark matter halo and a stellar disk. Each of these components is represented by collisionless N-body particles in the present study: the galactic potential is ‘live’ so that not only tidal effect of a MC-host dwarf on a MC but also dynamical friction of a MC against disk field stars of the dwarf can be self-consistently included. Therefore, the present study is more sophisticated and more realistic than our previous simulations of GC formation under a fixed galactic potential (e.g., Hurley & Bekki 2007; Bekki & Chiba 2007).

The present model for a dwarf galaxy is purely collisionless one, which means that gas dynamics, star formation, chemical evolution, and dust formation and evolution are not included at all, though the present simulation code enables us to investigate these physical processes. The dark matter halo with the total mass of  $M_{\text{h}}$  is represented by the ‘NFW’ one (Navarro et al. 1996) with a central cusp predicted by the Cold Dark Matter (CDM) model:

$$\rho(r) = \frac{\rho_0}{(r/r_s)(1+r/r_s)^2}, \quad (17)$$

where  $r$ ,  $\rho_0$ , and  $r_s$  are the distance from the center of the cluster, the central density, and the scale-length of the dark halo, respectively. The virial radius ( $r_{\text{vir}}$ ), the scale radius ( $r_s$ ), and the ‘ $c$ ’ parameter ( $=r_{\text{vir}}/r_s$ ) are chosen such that the values are consistent with recent cosmological simulations for the adopted  $M_{\text{h}}$  (Neto et al. 2007).

The dwarf is assumed to be as a bulge-less disk galaxy with the total stellar mass of  $M_{\text{s}}$  and the size of  $R_{\text{s}}$ . The radial ( $R$ ) and vertical ( $Z$ ) density profiles of the stellar disk are assumed to be proportional to  $\exp(-R/R_0)$  with scale length  $R_0 = 0.2R_{\text{s}}$  and to  $\text{sech}^2(Z/Z_0)$  with scale length  $Z_0 = 0.04R_{\text{s}}$ , respectively. In addition to the rotational velocity caused by the gravitational field of disk and dark halo components, the initial radial and azimuthal velocity dispersions are assigned to the disc component according to the epicyclic theory with Toomre’s parameter  $Q = 1.5$ . The vertical velocity dispersion at a given radius is set to be 0.5 times as large as the radial velocity dispersion at that point.

We investigate only one dwarf model in this study, because the main purpose of this paper is to investigate not the dynamical influences of MC-host dwarfs with different masses and types on star-forming MCs but the GC formation in fractal MCs. The dwarf galaxy is assumed to have  $M_{\text{h}} = 10^{10} M_{\odot}$ ,  $M_{\text{s}} = 6.0 \times 10^7 M_{\odot}$ ,  $R_{\text{s}} = 1.8$  kpc, and no gas. The mass and size resolutions for the simulation of the dwarf are  $6 \times 10^2 M_{\odot}$  and 25 pc, respectively. These resolutions are much lower than those for a MC with  $M_{\text{mc}} = 10^7 M_{\odot}$  ( $9.5 \times 10 M_{\odot}$  and 0.4 pc, respectively). In order to avoid unrealistically strong gravitational influences of clumpy distributions of dark matter and disk particles of a dwarf on the evolution of its MC, we adopt (i) multiple gravitational softening methods (Bekki & Tsujimoto 2016) and (ii) minimum time step width for numerically integrating different equations for the dwarf’s particles being the same as that for the MC.

The initial position ( $\mathbf{x}$ ) of a MC orbiting around its host dwarf is only a parameter for the tidal effects of MC-host dwarfs in the present study. The 3D position ( $x$ ,  $y$ , and  $z$ ) of a MC within a dwarf is given as follows:

$$\mathbf{x} = (r_{\text{p}}, 0, 0), \quad (18)$$

where  $r_{\text{p}}$  is the distance of the MC from the dwarf’s center. The MC is assumed to have a circular motion within the dwarf’s disk plane initially. Therefore, its 3D velocity ( $\mathbf{v}$ ) is given as follows:

$$\mathbf{v} = (0, v_{\text{c}}, 0), \quad (19)$$

where  $v_{\text{c}}$  is the circular velocity at the position  $\mathbf{x}$ . Accordingly,  $v_{\text{c}}$  is determined by the adopted live galactic potential of the dwarf. We investigate the models with  $r_{\text{p}} = 0.3$  and 1 kpc in the present study.

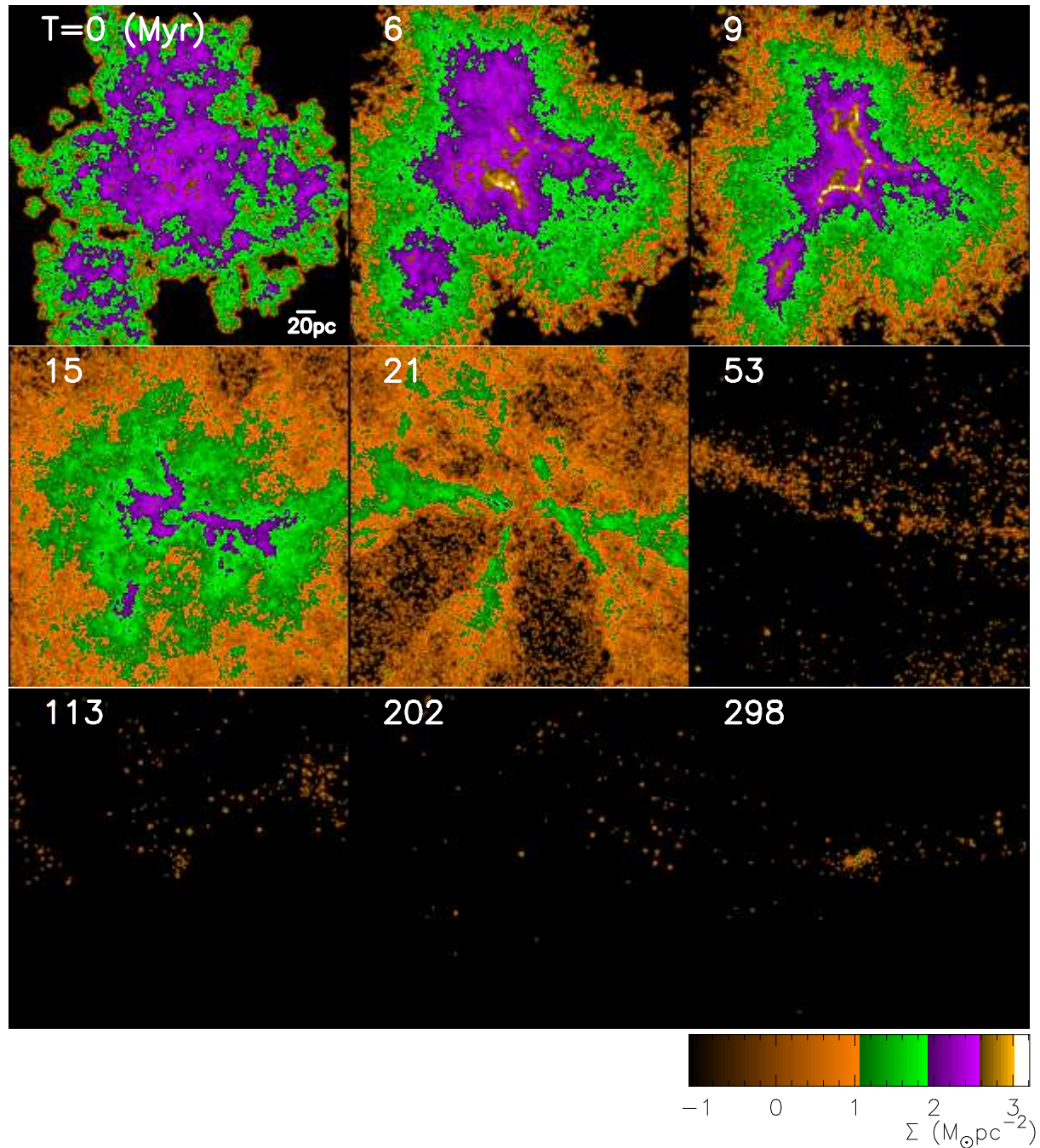


**Figure 1.** Time evolution of the surface mass density ( $\Sigma$ ) of original pristine gas projected onto the  $x$ - $y$  plane for the fiducial model with  $M_{\text{mc}} = 10^7 M_{\odot}$ ,  $R_{\text{mc}} = 200$  pc, and  $D_3=2$ . The time  $T$  at the upper left corner in each frame is given in units of Myr. A thick bar in each panel indicates a scale of 20 pc. For clarity, a color code in this figure is different from those used in Figs. 2, 3, and 4.

## 2.7 Parameter study

The key parameters for GC formation from fractal MCs are  $M_{\text{mc}}$ ,  $R_{\text{mc}}$ ,  $f_{\text{rot}}$ , and  $D_3$ , for a given IMF slope. Although other parameters such as initial radial density profiles of MCs and galactic potentials are also important, but we do not intend to discuss much about the roles of these parameters in GC formation. We mainly describe the results of the fiducial model in which  $M_{\text{mc}} = 10^7 M_{\odot}$ ,  $R_{\text{mc}} = 200$  pc,  $f_{\text{rot}} = 0$ , and  $D_3 = 2$ , because this model shows the typical behavior of GC formation with multiple generations of

stars within fractal MCs. The basic parameters used for the fiducial model is summarized in Table 2. We also discuss the results of other models with different values of the key parameters. The parameter values of all 38 models discussed in this paper are summarized in Table 3.

We focus mainly on the physical properties of the simulated GCs in models without SNe from SG stars, because it is expected that the total masses of SG stars ( $M_{\text{sg}}$ ) are unlikely to be as large as  $10^5 M_{\odot}$  owing to SF suppression by SNe in the models with SNe from SG stars (B11). How-

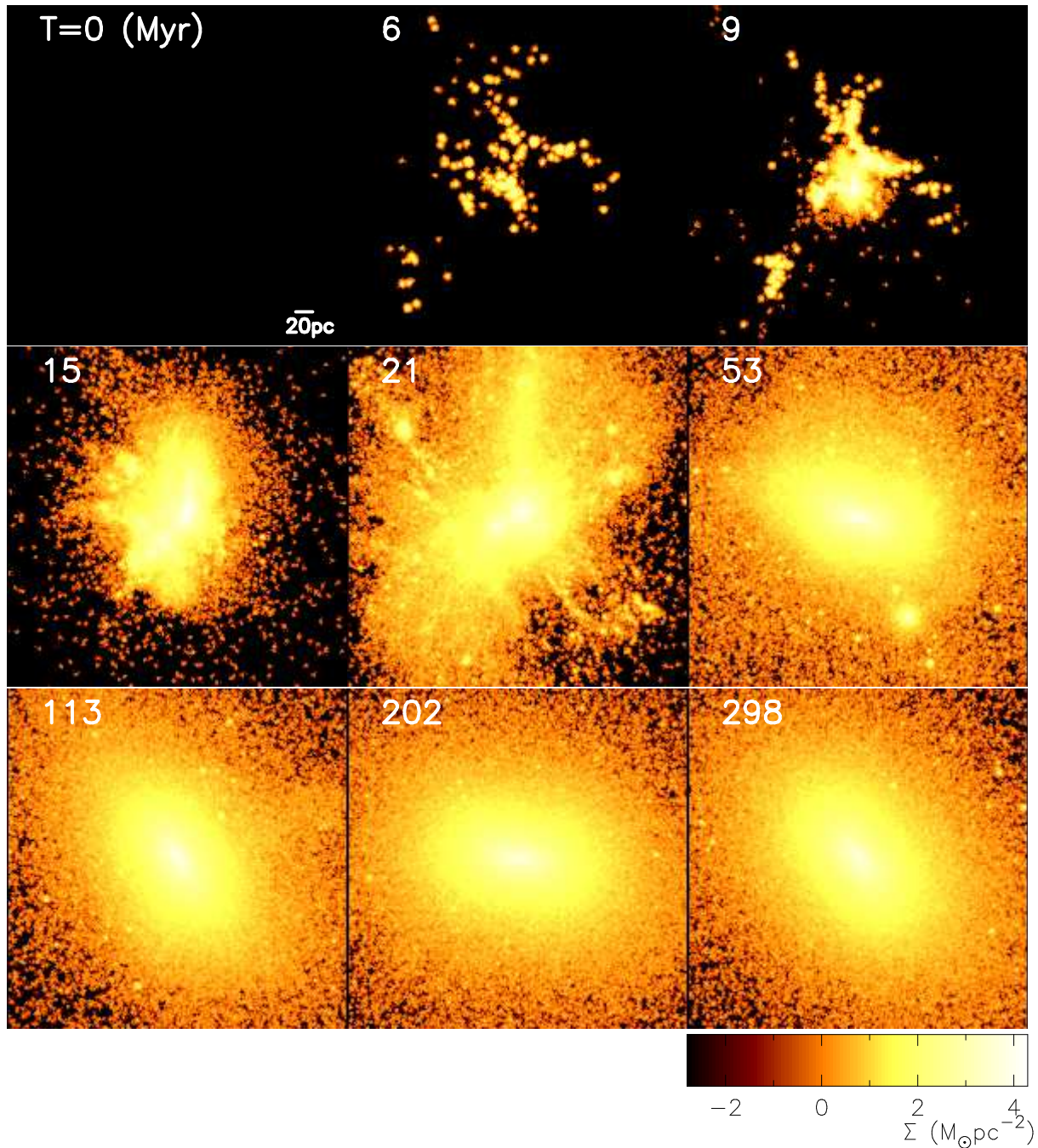


**Figure 2.** The same as Fig. 1 but for new stars formed from original gas ('FG' stars).

ever, we extensively investigate how SNe from SG stars can influence final  $M_{\text{sg}}$  of GCs using models with SNe from SG stars. We do not discuss the chemical abundances of simulated GCs so extensively in the present study, because the present paper already contains a substantial amount of new results and it is long. We accordingly discuss the chemical properties of the simulated GCs in our next paper using AGB and SN yields not only from K10 and T95 but also from other groups (e.g., Ventura et al. 2013). The results of models with ISM of dwarfs (i.e. possible gas that can dilute AGB ejecta) will be discussed in our forthcoming papers too.

### 3 RESULTS

#### 3.1 Dynamics of two-stage GC formation

Figs. 1-4 show how a massive GC consisting of FG and SG stars can be formed from a fractal MC in the fiducial model M1 with  $M_{\text{mc}} = 10^7 M_{\odot}$  and  $R_{\text{mc}} = 200$  pc and without SN feedback effect for stars formed from AGB ejecta. Numerous small gas clumps can be developed from local gravitational instability within the MC, and their local gas densities can become higher than  $10^4 \text{ cm}^{-3}$  ( $T = 6$  Myr). As a result of this, new stars can form in these gravitationally bound low-mass clumps ( $T = 9$  Myr) to become new low-mass SCs.

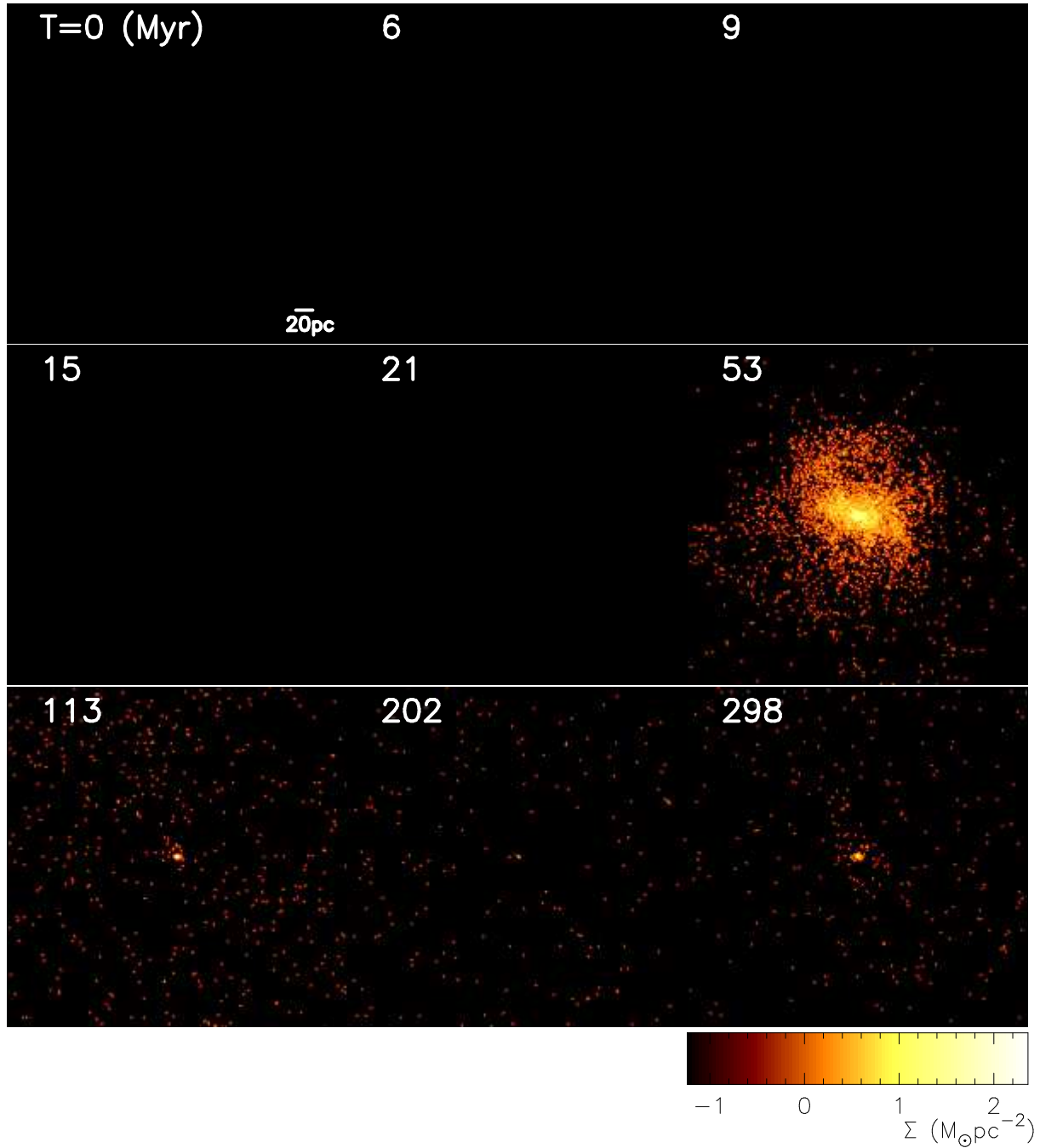


**Figure 3.** The same as Fig. 1 but for gas ejected from AGB stars of FG.

These new stars formed from pristine low-metallicity cold gas correspond to FG stars. The new SCs can merge with one another within the MC to form a single FG stellar system over the timescale of  $10^8$  yr. Star formation can proceed also in massive long filaments developed during the dynamical evolution of the fractal MC.

Multiple SN explosion can occur well before most of the cold gas is consumed by star formation, because SN explosion of massive stars with shorter lifetimes ( $< 10$  Myr corresponding to  $m_s > 30M_{\odot}$ ) are included in this fiducial model. Consequently, a significant fraction of cold gas that was not converted into new stars before SN explosion can be brown

away from the MC. Once cold gas is expelled from the MC ( $T = 21$  Myr), most of the gas can never be returned back to the inner part of the MC owing to the shallow gravitational potential (and to the non-inclusion of galactic potential). In the present fractal MC model, SN explosion can occur during merging of low-mass SCs, which is in striking contrast with SN explosion in the uniform distribution of cold gas in MCs. About 46% of initial cold gas can gain a large amount of momentum and be heated up so that the gas can be finally completely removed from the MC through SN explosion in this model. The final star formation efficiency of FG stars

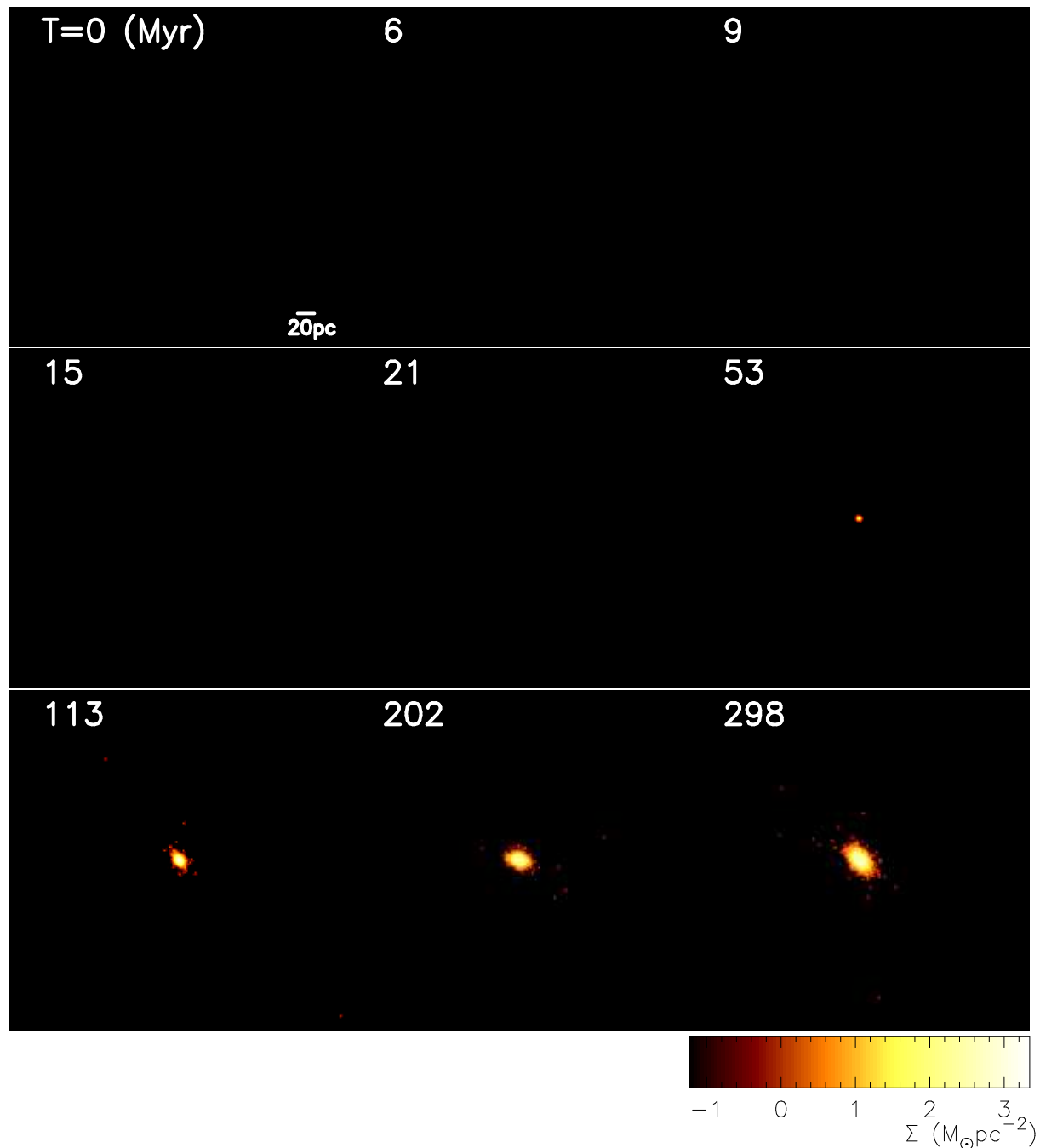


**Figure 4.** The same as Fig. 1 but for new stars formed from AGB ejecta of FG (‘SG’ stars).

( $\epsilon_{\text{fg}} \sim 0.5$ ) in this model is higher than 0.2–0.5 required for the formation of bound SCs (e.g., Hills 1980).

Chemical enrichment of pristine gas by SNe can proceed during multiple merging of low-mass SCs and new stars can be formed from such chemically polluted gas ( $T = 15, 21$  Myr). However, the fraction of the new stars is quite small, because almost all of the chemically polluted gas can be removed from the proto-GC region ( $R < 100$  pc) during GC formation. Furthermore such new star formation can occur well outside the inner region of the forming GC so that they can not be finally within the central region of the SG stellar system (i.e., the main component of the GC)

later formed. Thus it is not possible that the simulated GC can have significant internal abundance spreads in heavy elements (i.e.,  $\delta[\text{Fe}/\text{H}] > 0.05$  dex) between their stars within the central 5 pc.

After the removal of gas chemically polluted by SN explosion, massive AGB stars ( $m_s = [7 - 8]M_{\odot}$ ) start to eject Na-rich (He-rich) gas into the MC ( $T = 53$  Myr). Because of the relatively slow wind velocity ( $v_{\text{wind}} = 10 \text{ km s}^{-1}$ ), the AGB ejecta can be gravitationally trapped in the central region of the MC where a massive stellar system composed of FG stars only is developing ( $T = 53$  Myr). The AGB ejecta can be slowly accumulated in the inner region of the

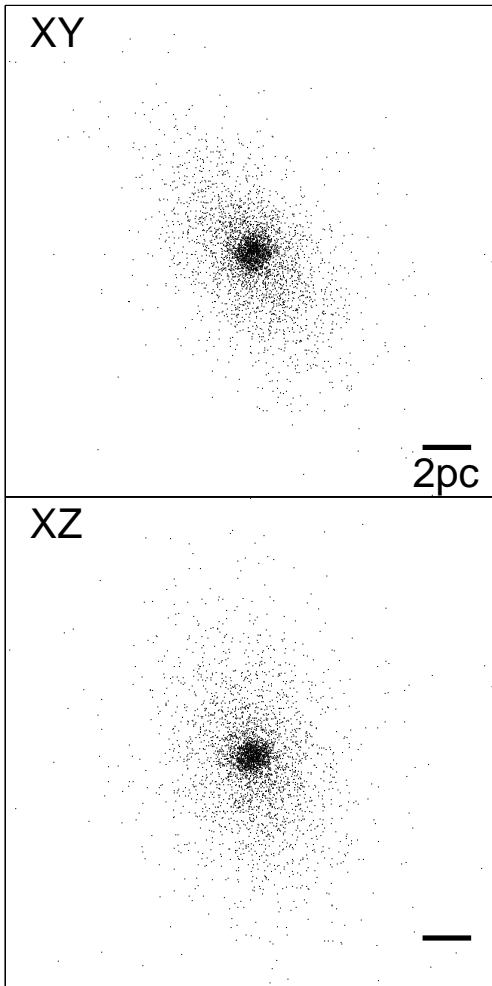


**Figure 5.** Mass distributions of SG stars projected onto the  $x$ - $y$  (upper) and  $x$ - $z$  planes (lower) at  $T = 113$  Myr in the fiducial model M1. A thick bar indicates a scale of 2 pc.

FG stellar system and finally converted into new stars when the gas density exceeds  $\rho_{\text{th}}$ . These new stars are SG in the MC and have a very compact spatial distribution initially. As shown in our previous works (B10, B11), this compact configuration is due largely to energy dissipation of gas during its accretion process. The SG stellar system is initially composed mostly of new stars formed from gas ejected from massive AGB stars with  $m_s \geq 6M_{\odot}$ . The SG system grows slowly by accretion of gas from AGB stars with lower  $m_s$  over a timescale of  $10^8$  yr. New SG stars formed from ejecta from AGB stars with lower masses can be distributed in the outer part of the SG system, which implies that He-rich SG stars has a more compact distribution than He-normal ones in a GC.

Although a significant fraction of AGB ejecta can be converted into new stars (SG), about 70% of the ejecta (in particle number) can not be converted into new stars in the central region of the forming GC. One of the physical reasons for this is that the ejecta can be influenced by energetic SNe: if SN explosions occur in the inner region of the forming GC, then the gas close to them can be expelled from

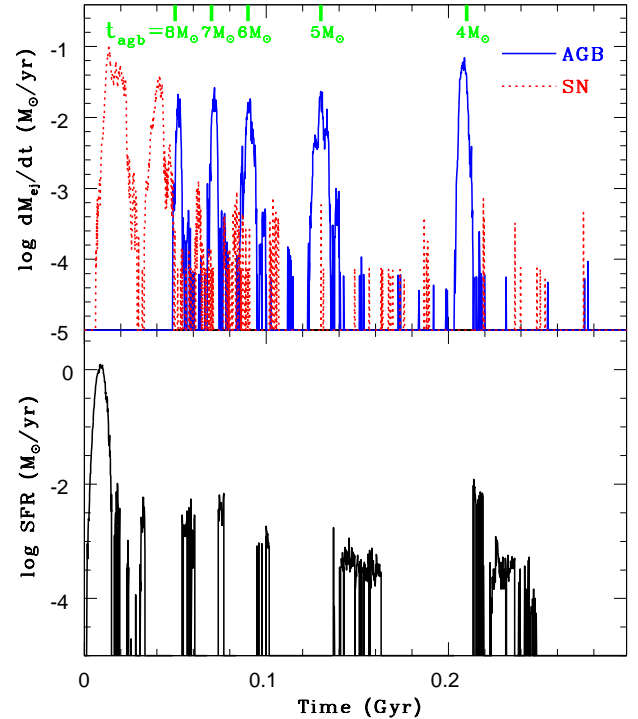


**Figure 6.** Time evolution of ejection rates of gas from SNe (red dotted) and from AGB stars (blue solid) in a proto-GC (upper) and the star formation history of the GC (lower) for the fiducial model. The epochs of gas ejection from AGB star ( $t_{\text{agb}}$ ) with different masses are shown by thick green lines at the top of the upper frame for the initial star burst around  $T = 5$  Myr in this model. Chemical pollution and feedback effects by SNe from SG stars are not included in this model. Therefore, all of SNe in this figure are from FG stars. Although most of the original gas can be expelled from the forming GC by  $T = 0.04$  Gyr, a very minor fraction of the gas can settle down to the inner region of the forming GC at later times, because the gas is not influenced by SN feedback effects (Only gas that is not influenced by SNe can stay in the inner region of the GC). SNe from FG stars formed later can suppress/truncate star formation, if the SNe occur in the central region of the forming GC during SG star formation there. AGB ejecta that is influenced by SNe (i.e., ejecta located close to SNe) can not stay in the central region of the forming GC. Accordingly, such ejecta is unlikely to form new stars: little self-enrichment in SG stars.

there. The other reasons is that the gas density is not so high as the adopted threshold gas density for star formation. Since discrete four epochs of SNe ( $t_{\text{sn}}$ ) are assumed in the present simulation, the influences of SNe on AGB ejecta could be under-estimated to some extent. It would be possible that gas ejected from AGB stars between interval of two discrete SN events can be accreted onto the central regions of GCs. However, such gas accretion is less likely because the differences of  $t_{\text{sn}}$  are typically small.

The derived timescale of SG formation that is much longer than the lifetime of massive stars that explode as massive SNe ( $\sim [3 - 10]$  Myr) imply that the formation of such massive stars need to be severely suppressed in SG star formation. The FG stellar system grown through merging of

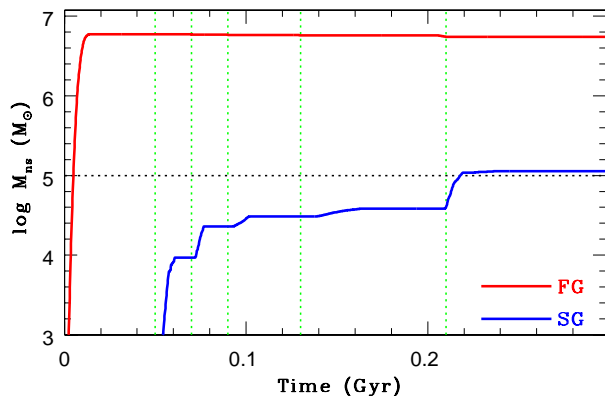


**Figure 7.** Time evolution of the total mass of FG (red) and SG (blue) stars in the fiducial model. The epochs of gas ejection of AGB stars with different masses are indicated by vertical green dotted lines, as shown in Fig. 1. A horizontal black dotted line shows the total masses of SG stars observed for typical old GCs of the Galaxy.

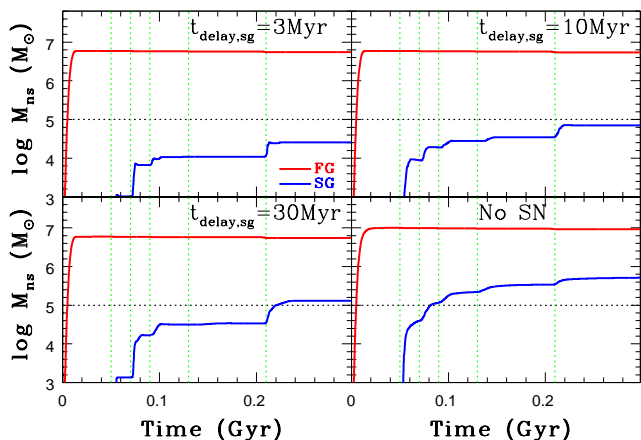


**Figure 8.** Time evolution of the total mass of FG (red) and SG (blue) stars in the models with  $t_{\text{delay,sg}} = 3$  Myr (upper right; M2),  $t_{\text{delay,sg}} = 10$  Myr (upper left; M3),  $t_{\text{delay,sg}} = 30$  Myr (lower left; M4), and no SN feedback in both FG and SG formation (lower right; M5). The epochs of gas ejection of AGB stars with different masses are indicated by green dotted lines, as shown in Fig. 1.

hierarchical star cluster complex in this model can finally have a very high mass ( $M_{\text{fg}} = 5.47 \times 10^6 M_{\odot}$ ). It has a more diffuse distribution and a large effective radius ( $R_{\text{e,fg}} \sim 25$  pc at  $T = 113$  Myr) whereas the SG stellar system has a very compact configuration with  $R_{\text{e,sg}} = 1$  pc. The mass ratio of SG to FG stars within the central 1 pc ( $= R_{\text{e,sg}}$ ) of the simulated GC at  $T = 113$  Myr is 1.9, which is consistent with the observed fraction of GCs (C09). The final total mass of the SG system is  $M_{\text{sg}} = 1.13 \times 10^5 M_{\odot}$ , which is roughly similar to the present typical total mass of SG stars (C09). Therefore, the mass ratio of SG to FG stars ( $f_{\text{sg}}$ ) is quite small ( $\sim 0.021$ ), though most of FG stars form an outer stellar halo around the simulated GC. The derived large  $M_{\text{fg}}$  means that the vast majority of FG stars should be

lost from the nested stellar systems, as discussed by several authors already (e.g., D08, B11, Vesperini et al. 2010). In the present fractal MC model, the initial MC mass should be quite large ( $M_{\text{mc}} \sim 10^7 M_{\odot}$ ), which is even larger than the mass ( $\sim 3 \times 10^6 M_{\odot}$ ) of the most massive giant molecular cloud (GMC) in the Galaxy (e.g., Solomon et al. 1987). This large required  $M_{\text{mc}}$  for GC formation within MCs might explain why the Galaxy currently does not have GCs in formation.

Although it is not straightforward to estimate the timescale of dynamical relaxation ( $t_r$ ) for the nested stellar system in the fiducial model, we can derive  $t_r$  separately for FG and SG stars using the formula by Spitzer & Hart (1971). The FG stellar system has  $t_r = 3.5 \times 10^{11}$  yr at  $R = 100$  pc (for  $M_{\text{fg}} = 5.47 \times 10^6 M_{\odot}$ ), which is much longer than the Hubble time. The SG system has  $t_r = 6.8 \times 10^8$  yr at  $R = 5$  pc (for  $M_{\text{fg}} = 1.13 \times 10^5 M_{\odot}$ ). The very long  $t_r$  of FG stars suggests that it is not possible for the entire FG and SG populations to be mixed well within  $\sim 10$  Gyr for the simulated GC, though the stars in the central region can be mixed together. Thus, the central region of the GC can be dominated by SG stars for a long timescale.

Fig. 5 shows that the simulated GC has an almost spherical distribution of SG stars in the inner 2pc with a more elongated (elliptical) outer halo of SG stars for the  $x$ - $y$  and  $x$ - $z$  projection. The spherical distribution can be due to no rigid rotation of the MC in this model. Fig. 6 demonstrates that there is a clear separation between the initial bursty formation of FG stars and the later sporadic formation of SG stars from gas of AGB stars with different masses. This is due largely to a combination of (i) efficient removal of remaining gas by SN explosion and (ii) long  $t_{\text{agb}}$  of AGB stars ( $> 4 \times 10^7$  yr). In the present model, continuous gas ejection from AGB stars with different masses can not be properly modeled owing to the strong limitation of gas particles numbers adopted in the simulations. Therefore, there are five peaks in the ejection rate ( $dM_{\text{ej}}/dt$ ) of gas from AGB stars, which correspond to the commencement of AGB phases of intermediate-mass stars with  $m_s = [7 - 8]M_{\odot}$ ,  $[6 - 7]M_{\odot}$ ,  $[5 - 6]M_{\odot}$ ,  $[4 - 5]M_{\odot}$ , and  $[3 - 4]M_{\odot}$ , respectively. Soon after each epoch of gas ejection from AGB stars, the star formation rate (SFR) for SG stars can significantly increase owing to the increased mass density of gas in the central region of the proto-GC. This apparently sporadic increase in SFR results simply from the adopted model for gas ejection from AGB stars in the present study: this should not be interpreted as the formation of discrete sub-populations within a single GC.

Fig. 6 shows that SN explosion is ongoing even when AGB stars are ejecting gas in the forming GC ( $T > 50$  Myr). Since SN explosion is not assumed to occur in stars formed from gas ejected from AGB stars (i.e., SG stars) in the fiducial model, all SNe in Fig. 6 are from FG stars. These FG stars are formed from (original) gas particles that were not influenced by SNe owing to its location being not close enough to SNe at earlier times ( $T < 40$  Myr). If original gas particles are influenced by SNe, then they gain energy and momentum and are chemically polluted by metals of the SNe. Accordingly, such gas particles can not settle down to the central region of the forming GC. Thus, gas particles that are later ( $T > 50$  Myr) converted into FG stars are much less chemically enriched by SNe. The time lag between

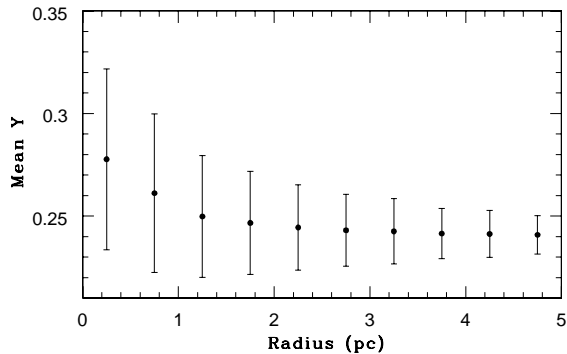


**Figure 9.** The projected radial profile of mean helium abundances ( $Y$ ) of GC stars (FG+SG) at  $T = 112$  Myr in the fiducial model. An error bar indicates the dispersion of  $Y$  in each bin.

gas ejection of AGB stars and SG star formation is rather short ( $< 3$  Myr), because accretion of AGB ejecta onto the inner region of the forming GC can rapidly proceed after almost all massive stars explode.

The formation of SG stars from AGB ejecta is possible, only if the ejecta is not located to the vicinity of a SN (i.e., only if it does not gain energy and momentum from the SN). AGB ejecta can be expelled from the forming GC if it is influenced by SN feedback effects. Accordingly, SG star formation at  $T > 50$  Myr in Fig. 6 is from AGB gas particles that are not influenced by SNe: The apparent coincidence of SN explosion and onset of AGB phase does not mean chemical pollution of AGB ejecta by SNe. It should be noted here that these later SNe are not necessarily located in the central region of the forming GC. SNe of FG stars formed later in the central region of the forming GC can expel the remaining AGB ejecta so that SG star formation can be severely suppressed or temporarily truncated.

A very small fraction of cold gas can not be completely ejected from the MC and therefore used for further star formation after its accretion onto the stellar system developing in the MC. This gas is not chemically polluted by SNe, because it is initially located in the outer part of the gas cloud (or because it is not located close to SNe). Given the pristine nature of the gas, AGB ejecta accumulated in the stellar system can be mixed with (or ‘diluted by’) the gas, though such dilution is not so efficient owing to the small mass of the gas. This dilution of AGB ejecta by pristine gas is one of essential ingredients of chemical evolution models for GCs with multiple stellar populations (e.g. Fenner et al. 2004; Bekki et al. 2007; D10), and the origin of such pristine gas has been discussed in previous works (e.g., D08, D10, B11, B17). The present study accordingly suggests that original cold gas that is not influenced by SN explosion can be used for dilution of AGB ejecta in forming GCs. However, the amount of such cold gas in the present study is too small (an order of  $\sim 10^4 M_\odot$ ) within the central 10pc of the proto-GC in comparison with the required one in previous models.

Fig. 7 demonstrates that  $M_{\text{sg}}$  can exceed  $10^5 M_\odot$  only after gaseous ejecta of low-mass AGB stars with  $m_{\text{agb}} = [3 - 4] M_\odot$  is accumulated onto the central region of the proto-GC and converted into new stars. This prolonged SG formation

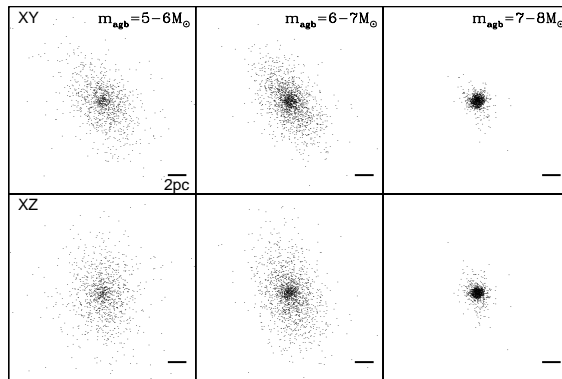


**Figure 10.** The same as Fig. 1 but for SG stars formed from gaseous ejecta of AGB stars with masses of  $[5 - 6] M_\odot$  (left),  $[6 - 7] M_\odot$  (middle), and  $[7 - 8] M_\odot$  (right),

over  $\sim 0.2$  Gyr in the MC can constrain the IMF of SG stars, as discussed later in this paper. The SFE of SG stars ( $\epsilon_{\text{sf,sg}}$ ) is 0.3 in this fiducial model, which suggests that the mass budget problem is even severer than ever thought in previous models in which  $\epsilon_{\text{sf,sg}}$  is assumed to be rather high. These results suggest that the threshold MC mass ( $M_{\text{mc,th}}$ ) beyond which typical GCs with  $M_{\text{sg}} \sim 10^5 M_\odot$  can be quite large:

$$M_{\text{mc,th}} \approx 10^7 M_\odot. \quad (20)$$

It should be stressed here that the original  $M_{\text{sg}}$  in GCs can be significantly larger than  $10^5 M_\odot$ , because GCs could have lost SG stars from tidal stripping and long-term internal dynamical processes driven by two-body dynamical relaxation. Thus,  $M_{\text{mc,th}}$  can be larger than the above value.

The SFE of FG stars in this model is high ( $\sim 0.5$ ), which is likely to be over-estimated, because the present study does not include suppression of star formation from original gas through ionizing photons and stellar winds of massive stars. These suppression effects are properly modeled in recent simulations of MC evolution (e.g., Dale et al. 2014). Since  $\epsilon_{\text{sf,fg}}$  can control the total mass of AGB ejecta from which SG stars can be formed, the present study without gas ionization and stellar winds of massive stars (before SNe) could also overestimate the total mass of SG stars in each simulated GC.

Fig. 8 shows that  $M_{\text{sg}}$  is smaller than  $10^5 M_\odot$  required for the formation of genuine GCs in the models (M2 and M3) with SNe from SG stars, if  $t_{\text{delay,sg}} \leq 100$  Myr. The model M2 with  $t_{\text{delay,sg}} = 3$  Myr shows  $M_{\text{sf}} = 2.6 \times 10^4 M_\odot$ , which implies that  $M_{\text{mc,th}}$  should be even significantly higher than  $10^7 M_\odot$  derived for M1. This result means that SNe from SG stars themselves can severely suppress the efficient conversion of AGB ejecta into new stars, because energetic SN feedback effects blow away the ejecta from the central region of the proto-GC. This furthermore suggests that the formation of high-mass SNe with short lifetimes ( $\leq 100$  Myr) from SG stars need to be truncated for the formation of GCs with  $M_{\text{sg}} > 10^5 M_\odot$ . This result implies that the upper-mass cutoff of the IMF for SG stars needs to be quite low ( $< 10 M_\odot$ ) for the efficient formation of SG stars from AGB ejecta ( $\epsilon_{\text{sf,sg}} \sim 0.3$ ). The simulated GC can have  $M_{\text{sg}} > 10^5 M_\odot$  in the early phase of GC formation ( $T < 0.1$

Gyr) in the model (M5) without SNe from FG and SG stars, because AGB ejecta can be quickly accreted onto the central region of the GC without being influenced by SN feedback effects.

As shown in Fig. 9, the simulated GC in the fiducial model has a negative radial gradient of helium abundance ( $Y$ ) within the central 3 pc of the GC. The higher  $Y$  in the inner region results from the higher mass fraction of SG stars with higher  $Y$  due to their more compact distribution. The dispersion in  $Y$  is also higher in the central region, which reflects the fact that new stars can be formed from gaseous ejecta from AGB stars with different masses and thus different  $Y$ . The outer part of the simulated GC is dominated by FG stars with  $Y = 0.24$  so that the dispersion in  $Y$  can be rather small. These negative  $Y$  gradient and higher dispersion in  $Y$  in the inner region of the simulated GC can be seen in almost all massive MC models of the present study. The adopted simulation code does not allow us to discuss the long term ( $> 10^9$  yr) dynamical evolution of a GC through two-body relaxation processes. Accordingly, it remain unclear whether the derived negative radial gradients of  $Y$  in the simulated GCs can persist for  $10^{10}$  yr. It could be possible that such initial  $Y$  gradients can be kept as they are in massive GCs with long relaxation timescale, such as  $\omega$  Cen.

In the present model of GC formation, gaseous ejecta from more massive AGB stars can be accumulated onto a diffuse FG stellar system earlier so that it can be converted into a very compact stellar system. Most gaseous ejecta from less massive AGB stars can not reach the very central region of the forming GC, instead, it can be accreted later onto the surrounding region of the compact SG stellar system formed earlier (the ejecta forms a disk structure). As a result of this, SG stars formed from low-mass AGB stars have more diffuse spatial distributions. Fig. 10 clearly demonstrates that SG stars formed from massive AGB stars with masses of  $[7 - 8]M_{\odot}$  have a more compact distribution. If more massive AGB stars with  $[7 - 8]M_{\odot}$  can eject gas with higher  $Y$  than less massive ones with  $[5 - 6]M_{\odot}$ , then this result in Fig. 10 implies that there can be differences in the spatial distributions between SG stars with different  $Y$ . The chemical yield model of AGB stars from K10 adopt in the present study predicts such a trend of increasing  $Y$  with increase AGB star mass.

### 3.2 Parameter dependence

Formation processes of GCs (i.e., ‘two-stage’ FG and SG star formation) and physical roles of feedback effects of SNe and AGB stars in star formation histories (SFHs) of GCs are essential the same between different models. However, the details of the two-stage GC formation processes and SFHs depend on model parameters. Furthermore,  $M_{\text{sg}}$  in some models with lower  $M_{\text{mc}}$  is too small for the simulated GCs to be identified as GCs with multiple stellar populations. Such GCs dominated by FG stars are regarded as ‘failed GCs’ in the present study and might be better labeled as low-mass SCs. The time evolution of  $M_{\text{fg}}$  and  $M_{\text{sg}}$  and final  $M_{\text{sg}}$  and  $\epsilon_{\text{sf,sg}}$  for representative models in the present study are summarized in Figs. 11 and 12, respectively. The dependences of the present results on the model parameters

are summarized as follows.

(1) As shown in Fig. 11, only some of the very massive MC models with  $M_{\text{mc}} = 10^7 M_{\odot}$  can show  $M_{\text{sg}} \approx 10^5 M_{\odot}$ , which is required for the present-day typical GCs. This result suggests that there is a threshold MC mass beyond ( $M_{\text{mc,th}}$ ) which GCs can be formed from MCs. Even the simulated GCs in the models with  $M_{\text{mc}} = 3 \times 10^6 M_{\odot}$  can not have SG stellar systems with  $M_{\text{sg}} \approx 10^5 M_{\odot}$ . This means that even the most massive Galactic MCs with  $M_{\text{mc}} = 3 \times 10^6 M_{\odot}$  (e.g., Solomon et al. 1987) are unlikely to form GCs. Thus the possible presence of  $M_{\text{mc,th}}$  is a physical reason why the Galaxy is currently not forming massive GCs.

(2) The simulated SCs (or ‘failed GCs’) in the models with  $M_{\text{mc}} = [1 - 3] \times 10^6 M_{\odot}$  (M19 - M35) can contain SG stars, however, both  $f_{\text{sg}}$  and  $\epsilon_{\text{sf,sg}}$  are significantly lower than those derived for the models with  $M_{\text{mc}} = 10^7 M_{\odot}$ . These results imply that  $f_{\text{sg}}$  can be quite diverse, however, the observed  $f_{\text{sg}}$  is not so diverse (C09). Although the results only for three models are shown in the present study (Table 1 and Fig. 11), it is confirmed that simulated SCs in the models with  $M_{\text{mc}} = 3 \times 10^5 M_{\odot}$  (M36 - M38) do not contain SG stars at all for models with different parameters. Such an inability of SG star formation in low-mass MC results from the fact that AGB ejecta can not form high-density gaseous regions within stellar systems composed of FG stars. A significant fraction AGB ejecta with a wind velocity of  $10 \text{ km s}^{-1}$  can escape from the low-mass MCs with shallower gravitational potentials. The final SCs in these models can not be regarded as genuine GCs, and they are more similar to open clusters with single stellar populations.

(3) Compact stellar systems with  $M_{\text{sg}} \sim 10^5 M_{\odot}$  can be formed within MCs with  $M_{\text{mc}} = 10^7 M_{\odot}$ , regardless of whether they have initial rotation (M6). However,  $\epsilon_{\text{sf,fg}}$  and  $\epsilon_{\text{sf,sg}}$  in the rotating MC model M6 are slightly smaller than those in M1 without rotation. This less efficient SF in FG and SG stars in rotating MCs can be seen in models with different  $M_{\text{mc}}$  (e.g., M21 and M22). This suggests that initial rotation of GC-hosting MCs can also control  $M_{\text{fg}}$  and  $M_{\text{sg}}$  and thus the present-day masses of GCs. It should be also noted here that binary GCs can be formed in the models with  $f_{\text{rot}} \geq 0.1$  in some low-mass MC models. This binary SC formation in fractal MCs will be discussed in our forthcoming papers.

(4) Regardless of  $M_{\text{mc}}$ , the two-stage GC formation process does not depend strongly on  $D_3$  (e.g., M7 vs M8 for  $M_{\text{mc}} = 10^7 M_{\odot}$ ). The suppression of SG star formation by SNe from SG stars and the resultant lower  $M_{\text{sg}}$  can be clearly seen in the models with  $D_3 = 2.4$  for  $M_{\text{mc}} = 10^7 M_{\odot}$  (M8 vs M9),  $M_{\text{mc}} = 3 \times 10^6 M_{\odot}$  (M23 vs M24), and  $M_{\text{mc}} = 10^6 M_{\odot}$  (M33 vs M34). Here the results in the models with  $D_3 = 2.4$  are not described for  $M_{\text{mc}} = 3 \times 10^5 M_{\odot}$ , simply because they do not show any SG star formation. These results for  $D_3 = 2.4$  combined with those for  $D_3$  demonstrate that SN feedback effects are the most important physical effect for SG formation. These

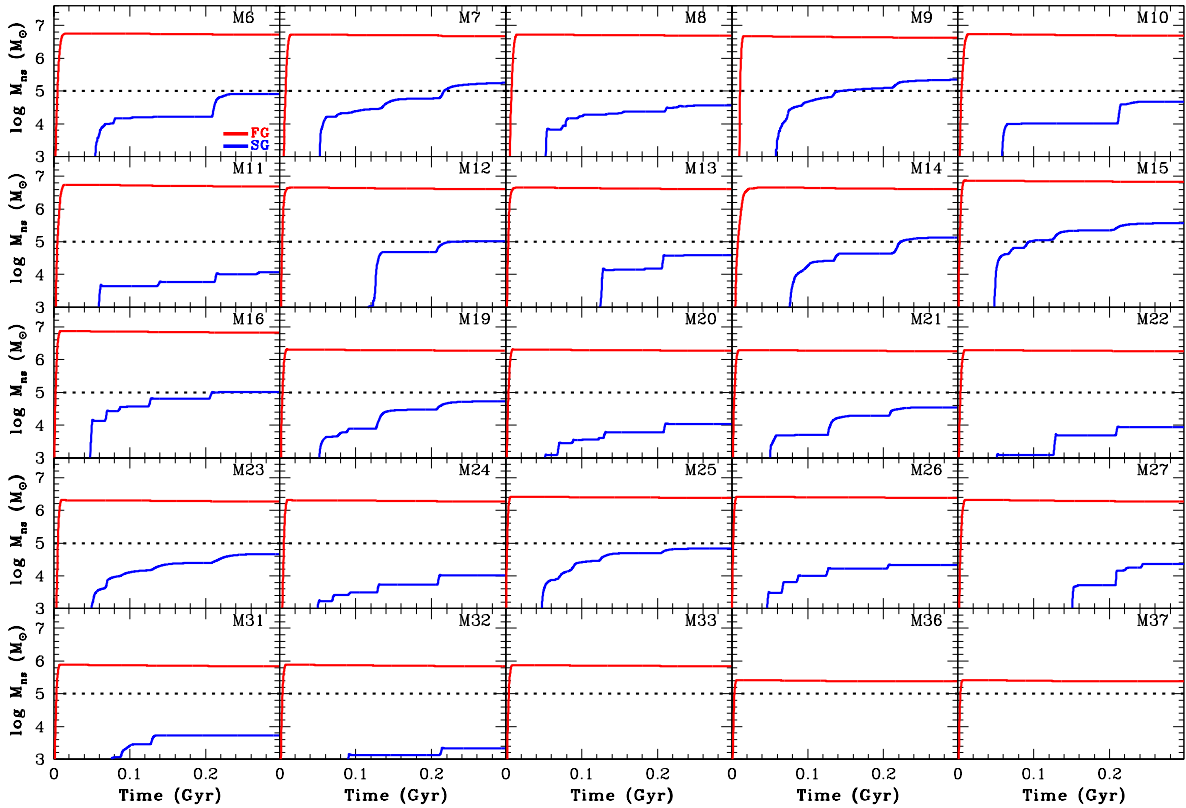


**Figure 11.** The same as Fig. 7 but for 25 representative models in the present study. The model ID is given in the upper right corner of each panel. 25 models are selected from 38 investigated in the present study.

also imply that the IMF for the SG star formation should be top-light (almost no massive SNe) for GCs to have significant fractions of SG stars. This point is discussed later in this paper.

(5) Threshold densities for star formation ( $\rho_{\text{th}}$ ) can also control the time evolution of  $M_{\text{fg}}$  and  $M_{\text{sg}}$  in the sense that  $M_{\text{fg}}$  and  $M_{\text{sg}}$  can be smaller for larger  $\rho_{\text{th}}$  for models with different  $M_{\text{mc}}$ . The final  $M_{\text{sg}}$  can be significantly smaller in the models with  $\rho_{\text{th}} = 10^5$  than in those with  $\rho_{\text{th}} = 10^4$  (i.e., strong suppression of SG formation). Although this is initially expected for the adopted star formation model, this has some implications on GC formation, which is discussed later in this paper. MCs with higher initial mass densities can show larger  $M_{\text{sg}}$  (e.g., M14 vs M15). The high-density massive MC model M16 with SNe from SG stars show  $\epsilon_{\text{sf,sg}} = 0.24$  and  $M_{\text{sg}} = 1.0 \times 10^5 M_{\odot}$ . This result implies that if massive MCs have rather high initial densities, then SNe from SG stars can not so strongly suppress SG star formation.

(6) The strong tidal field of a MC-host dwarf galaxy does not so strongly influence the formation processes of GCs. Compact SG systems can be formed from AGB ejecta in the models with galactic tidal fields (M17, M18, M29, and M30). Final  $M_{\text{sg}}$  and  $\epsilon_{\text{sg}}$  in the models with galactic tidal fields are appreciably smaller than those without. For example,  $\epsilon_{\text{sf,sg}}$  is 0.12 for  $r_{\text{p}} = 0.3$  kpc (M17) 0.21 for  $r_{\text{p}} = 1$  kpc (M18). Galactic tidal fields can be important

for disintegrating the more diffuse FG stellar systems, as suggested by previous numerical simulations of GC formation (D08 and B11). The present models with and without galactic tidal fields show a correlation between  $M_{\text{sg}}$  and  $\epsilon_{\text{sf,sg}}$  (See Fig. 12). This is due partly to SFE of SG stars being higher in MCs with higher masses.

(7) As shown in Fig. 13 for the fiducial model, GC stars do not show large metallicity spreads in the simulated massive Gs. SG stars show a smaller metallicity spread than FG stars, because they can be formed from almost pure AGB ejecta without significant chemical pollution by SNe. However,  $\Delta[\text{Z}/\text{H}]$  can be as large as 0.04 dex for FG stars. Fig. 13 shows that  $\Delta[\text{Z}/\text{H}]$  of GC stars (FG+SG) within 20 pc is slightly larger than the observed  $\Delta[\text{Z}/\text{H}]$  ( $< [0.02 - 0.03]$  dex) for 17 Galactic GCs (Caretta et al. 2010). Gas remaining in the outer part of the the GC ( $R > 20$  pc) shows a large metallicity spread, because the gas was expelled by SNe after being chemically polluted by SNe. It is not observationally clear whether FG stars show a larger  $\Delta[\text{Z}/\text{H}]$  than SG stars in a GC, as predicted in the present study. If FG stars in observations do not show larger  $\Delta[\text{Z}/\text{H}]$ , then the present model would need to be revised in terms of chemical pollution of original gas by SNe.

(8) In the present parameter study, mixing of AGB ejecta with SN ejecta is not so well resolved in all models, because the minimum number of AGB particles (or any gas particles) around one SN is set to be 8. This could cause an under-estimation of SN effects on AGB ejecta. For example,

the present study could have over-estimated  $M_{\text{sg}}$  and under-estimated the metallicity spreads among SG stars owing to the possible under-estimation of the mixing of SN and AGB ejecta. This issue will need to be discussed in our future simulations with a much better spatial resolution for the interaction between SN and AGB ejecta. The potential problem of AGB ejecta being contaminated by hot gas from SNe has not been convincingly (and fully) solved in the present study with a spatial resolution of an order of 0.1pc.

## 4 DISCUSSION

### 4.1 Necessity of top-light IMF in SG star formation in self-enrichment scenarios

Most old globular clusters (GCs) in the Galaxy to have star-to-star abundance spreads in light elements (e.g., C, N, and O) and the observed Na-O anti-correlation has been considered to be one of the characteristic features of GCs (e.g., C09). If the majority (70%) of stars with enhanced Na and depleted O (i.e., SG stars) are formed from gas ejected from FG stars with normal Na and O, then the original total mass of FG stars in a GC can be inferred from the present-day total mass of SG stars ( $M_{\text{sg}}$ ). Previous studies suggested that  $M_{\text{fg}}$  should be much more massive than  $M_{\text{sg}}$  (i.e., the mass budget problem). In the following, we discuss this mass budget problem in the context of self-enrichment scenarios based on SG formation from AGB ejecta.

The mass budget problem can be formulated as follows (B17):

$$M_{\text{fg}} = 1.4 \times 10^7 \left( \frac{\epsilon_{\text{sf,sg}}}{0.1} \right)^{-1} \left( \frac{f_{\text{ej,fg}}}{0.1} \right)^{-1} \left( \frac{M_{\text{sg},0}}{1.4 \times 10^5 M_{\odot}} \right) M_{\odot}, \quad (21)$$

where  $f_{\text{ej,fg}}$  is the mass fraction of gas ejected from AGB stars of FG and the star formation efficiency in SG star formation ( $\epsilon_{\text{sf,sg}}$ ) is assumed to be 0.1, as shown in the models with SN feedback effects on SG star formation. As long as a canonical IMF is assumed, such a small  $f_{\text{ej,fg}}$  and SN feedback effects on SG formation (i.e., low  $\epsilon_{\text{sf,sg}}$ ) are inevitable outcomes. The derived  $M_{\text{fg}}$  is underestimated to some extent, because mass loss of SG AGB stars are not considered. Nevertheless  $M_{\text{fg}}$  appears to be too large, which means that 99% of FG stars needs to be lost to form GCs with the observed mass fractions of FG and SG stars. Thus, if the IMF of SG stars is a canonical one, then the mass budget problem is much more severe than ever thought.

The mass budget problem can be less severe, if the IMF of FG stars is top-heavy (i.e., a larger fraction of AGB stars thus a higher  $f_{\text{ej}}$ ) and if the IMF of SG stars are top-light (i.e., a smaller fraction of SNe). Probably, the formation of massive SNe with shorter lifetimes need to be completely shut down to alleviate the mass budget problem. Such suppression of massive star formation was already pointed out by D08, though they did not discuss this in a quantitative manner. A key question in any self-enrichment scenarios is therefore whether or not the formation of massive stars ( $m_s \geq [30 - 120] M_{\odot}$ ) can be really severely suppressed (i.e., ‘top-light’ IMF) in SG star formation. Although our previous simulations of SG formation in dense stellar systems of FG stars investigated star formation processes (B10, B11), the IMF of SG stars could not be investigated owing to the adopted resolution. It is accordingly our future theoretical

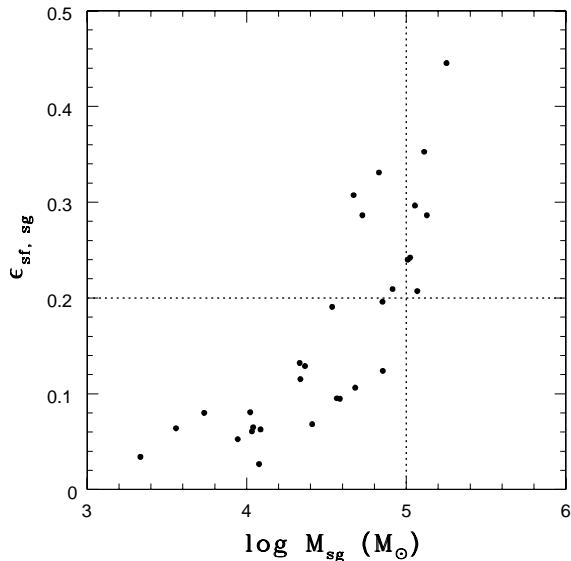


**Figure 12.** Star formation efficiencies (SFEs) of SG stars ( $\epsilon_{\text{sg}}$ ) as a function of  $M_{\text{sg}}$  for all models investigated in the present study. The vertical and horizontal dotted lines represent the observed typical mass of SG stars in the Galactic GCs and the threshold SFE (0.2) above which bound clusters can be formed from gas clouds (e.g., Hills 1980; Elmegreen & Efremov 1997).

study to investigate the slope and the upper-mass cutoff of the IMF for SG stars using numerical simulations that resolve star-forming cores. If our future study on this issue reveals that there is no plausible theoretical reason for the top-light IMF of SG stars, then we would need to discard self-enrichment scenarios as a major mechanism of GC formation.

### 4.2 If self-enrichment scenarios are not viable, then why can not secondary star formation occur ?

If self-enrichment scenarios based on gaseous ejecta from AGB stars are not viable for GC formation with multiple stellar populations, then it needs to be clarified why secondary star formation can not occur in forming GCs with a plenty of AGB ejecta. As shown in previous theoretical works on the formation of massive GCs, gaseous ejecta of AGB stars can be well retained in the central regions of the GCs (D08 and B11). Therefore, some physical mechanisms need to operate so as to suppress conversion from gas into new stars in dense stellar systems. Recent galaxy-scale numerical simulations of star formation histories in luminous and dwarf disk galaxies have demonstrated that star formation can be severely suppressed by photo-electric heating (PEH) of cold gas by dust (Bekki 2015; Forbes et al. 2016). The gas accumulated onto FG stellar systems from AGB stars can be dust-rich so that PEH effects can be strong if there is an enough amount of stellar radiation from FG stars in the central regions of proto-GCs. However, if AGB ejecta is diluted by pristine metal-poor gas, which is required for chemical evolution model of GCs, then such PEH effect could be weak. Accordingly, we need to investigate how such

PEH effect can influence the secondary star formation processes in proto-GCs.

It would be also possible that high number densities of stars in proto-GCs can totally prevent gravitational instability of gas that leads to star formation. The spatial resolution ( $\sim 0.4$  pc) of the present simulation is not good enough to investigate the very small-scale ( $\ll 1$  pc) formation processes of each individual stars. If dense stellar environments can really prevent secondary star formation, then it needs to be understood how and where AGB ejecta can be lost in proto-GCs. Ram pressure stripping of AGB ejecta by warm and hot ISM of GC-host galaxies could be a candidate mechanism for the removal of AGB ejecta, if proto-GC can pass through such ISM. It might be also possible that GCs can lose their AGB ejecta by ram pressure when they orbit around the halos of their host luminous galaxies like the Galaxy. If self-enrichment scenarios need to be discarded, a crucial question is when GCs achieved star-to-star internal abundance spreads during their formation histories. One idea is that new stars of proto-GCs already had star-to-star internal abundance spreads before their first SNe explode. It is not clear, however, how such chemical enrichment can proceed within  $\sim 3$  Myr (before first massive SNe explode).

It should be noted here that the above discussion is based on secondary star formation of gas ejected from AGB stars. An alternative self-enrichment scenario based on gaseous ejecta from fast-rotating massive stars (FRMS) has been already discussed by several authors (e.g., Decressin et al. 2007). This FRMS self-enrichment scenario has no problem associate with later SNe that can severely suppress secondary star formation. However, it is not clear in this FRMS scenario how SG star formation can be completed well before SN explosions of FG stars, which can expel all of the remaining gas within GC-forming molecular clouds. We here do not discuss how to avoid this potentially serious problem, because it is beyond the scope of this paper to investigate the FRMS scenario in detail. in detail.

### 4.3 Metallicity spreads in GCs

Although Lee et al. (2009) investigated the color magnitude diagrams ( $V$  vs  $b - y$  or  $hk$ ) of the Galactic GCs and found evidence of Ca abundance spreads in the 7 GCs, Carretta et al. (2010) showed that Ca abundance spreads among FG and SG stars in 17 Galactic GCs are less than 0.02 – 0.03 dex. The most massive Galactic GC  $\omega$  Cen and 8 GCs (e.g., M22) have been observed to show  $[\text{Fe}/\text{H}]$  spreads among GC stars so far (e.g., Freeman & Rodgers 1975; Marino et al. 2015). The apparent lack of internal  $[\text{Fe}/\text{H}]$  spreads among GC stars in most GCs implies that self-enrichment by SNe did not proceed efficiently at GC formation for some physical reasons. Since these GCs show anti-correlations between light elements, which could be due to self-enrichment by AGB stars, the physical mechanisms that suppress self-enrichment by SNe in GC formation need to be understood clearly. Nakasato et al. (2000) investigated star formation histories of proto-GC clouds with the masses of  $10^6 M_{\odot}$ , sizes of 150 – 300 pc, and initial temperature of  $10^4$  K using their original SPH simulations with feedback effects chemical enrichment by SNe. They found that although star formation in shell-like gaseous structures formed through com-

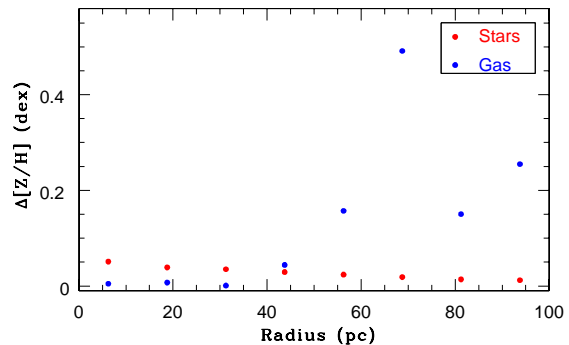


**Figure 13.** Internal metallicity spreads ( $\Delta[\text{Z}/\text{H}]$ ) for GC stars (red) and gas (blue) as a function of radius ( $R$  from the GC center) in the simulated massive GC for the fiducial model. The internal  $[\text{Z}/\text{H}]$  spread of gas is smaller than that of the stars for  $R < 20$  pc, because only the gas that is not chemically polluted (not expelled by SNe) can remain in the central region of the GC. The  $[\text{Z}/\text{H}]$  spread for SG stars formed from such gas (less chemically contaminated by SNe) can be smaller than that of FG stars. The  $[\text{Z}/\text{H}]$  spread of gas in the outer part of GC is significantly larger than that of the stars ( $R > 60$  pc), because the gas is the AGB ejecta expelled by SN explosions after being chemically polluted by SNe. The  $[\text{Z}/\text{H}]$  spread of GC stars is slightly larger than the observed small spread ( $< [0.02 - 0.03]$  dex) by Carretta et al. (2010).

pression of gas through SNe feedback effects is possible, self-enrichment is not seen to occur in all of their models.

The present study have demonstrated that although new star formation from gas contaminated by SNe is possible, the mass fraction of such stars is quite small. Furthermore, most of such stars can be formed mostly in the shocked gas that are distant from the main GC-forming regions, and therefore they can not be finally within the central regions of GCs. As a result of this, the mass fraction of such (SG) stars with  $[\text{Fe}/\text{H}]$  by more than 0.05 dex larger than (FG) stars formed from original cold gas of GC-forming GCs is quite small within the central 10pc of GCs. This implies that the apparent lack of  $[\text{Fe}/\text{H}]$  spreads in typical GCs is due largely to SN feedback effects in GC-forming MCs. Baumgardt et al. (2008) shows that the stellar masses of GCs required for self-enrichment by SNe is more than  $10^7 M_{\odot}$ , which means that original GC-hosting MC should be very massive ( $\sim 10^8 M_{\odot}$ ) for a reasonable star formation efficiency ( $\sim 0.1$ ). Therefore, typical GCs are unlikely to have  $[\text{Fe}/\text{H}]$  spreads.

The most massive Galactic GC  $\omega$  Cen has been suggested to originate from a nucleated dwarf galaxy (e.g., Freeman 1993; Bekki & Freeman 2002), where its deep potential well could retain ejecta from SNe for further star formation. Although other eight ‘anomalous’ GCs with  $[\text{Fe}/\text{H}]$  spreads could be also from defunct nucleated dwarfs like  $\omega$  Cen, it remains unclear what physical mechanisms are responsible for their  $[\text{Fe}/\text{H}]$  spreads. One of intriguing observational results is that some of anomalous GCs with metallicity spreads (e.g., M22) also show abundance spreads in  $s$ -process elements (Marino et al. 2011). The observed spreads in  $s$ -process elements could be due to star formation from gas polluted by AGB stars. The present study has shown that

SG stars have the same metallicities as those of FG stars, because SG stars can be formed from AGB ejecta only after SN explosion expel the remaining gas of MCs. Therefore it appears unlikely that simple self-enrichment scenarios can explain the origin of abundance spreads both in  $[\text{Fe}/\text{H}]$  and  $s$ -process elements.

Bekki & Tsujimoto (2016) have recently demonstrated that merging between massive GCs with initially different  $[\text{Fe}/\text{H}]$  in their host dwarf galaxy is possible, which ends up with a bimodal  $[\text{Fe}/\text{H}]$  distribution that is consistent with observations for M22 (Marino et al. 2011). They suggested that other anomalous GCs could be also formed from GC merging within dwarf galaxies with different star formation histories. It could be possible that only very massive GCs like  $\omega$  Cen experienced self-enrichment by SNe at their formation:  $[\text{Fe}/\text{H}]$  spreads in GCs alone do not necessarily mean star formation from gas polluted by SNe within their host MCs. Although GC merging is a promising mechanism for the origin of anomalous GCs, it has not reproduced several chemical abundances of their stars in a fully self-consistently manner (e.g., abundance spreads in C+N+O). Thus, there are still puzzling observational results on these GCs, which need to be addressed in our future papers.

## 5 CONCLUSION

We have investigated the formation processes of GCs with multiple stellar populations within massive molecular clouds (MCs) with fractal structures using our original hydrodynamical simulations with star formation, feedback effects of SNe and AGB stars, and chemical enrichment by these stars. The key parameters of the simulations are the masses ( $M_{\text{mc}}$ ), sizes ( $R_{\text{mc}}$ ), ratios of rotational energy to total kinetic energy ( $f_{\text{rot}}$ ) and fractal dimensions ( $D_3$ ) of GC-forming massive MCs. We have analyzed the physical properties of new stars formed from original pristine gas (first generation of stars; ‘FG’) and from gaseous ejecta of AGB stars (second generation; ‘SG’). We have also investigated (i) the models with and without SN feedback effects in the formation of SG stars (ii) those in which tidal field of dwarf galaxies hosting GCs are included. The principal results are as follows:

(1) Bound massive clusters of FG stars can be first formed from merging of hierarchical star cluster (SC) complexes that are developed from fractal gaseous structures of massive cold MCs with  $M_{\text{mc}} = 10^7 M_{\odot}$ . During merging of low-mass SCs within MCs, gas ejected from SNe can interact with the surrounding pristine gas of GC-forming MCs. SNe of very massive stars with  $m_s = [60 - 120] M_{\odot}$  can blow off cold gas from the very early stage of GC formation. After almost all of the cold gas is expelled from proto-GCs by SNe with different masses, gas ejected from AGB stars can be accumulated into the central regions of proto-GCs, where the AGB ejecta is converted into SG stars. This formation process of SG stars from AGB ejecta is consistent with the results of our previous 3D hydrodynamical simulations of GC formation (B10, B11).

(2) Most SG stars can be formed from gaseous ejecta in the central regions of FG stellar systems for all massive MC

models. The spatial distributions of SG stars are therefore initially more compact than those of FG stars in GCs for all models with different parameters. Since SG stars can be formed from ejecta of AGB stars with different masses, there can be significant differences in chemical abundances between SG stars. GC stars (FG and SG) show negative gradients of helium ( $Y$ ) abundances (i.e., higher  $Y$  in the inner regions) within the central 3 pc of the simulated GCs. SG stars formed from high-mass AGB stars ( $m_s = 7 - 8 M_{\odot}$ ) are more centrally concentrated than those from low-mass ones ( $m_s = 4 - 5 M_{\odot}$ ). This suggests that there is significant differences in spatial distributions between SG stars with different helium abundance ( $Y$ ), because high-mass AGB stars can eject gas with higher  $Y$ .

(3) There is a threshold MC mass ( $M_{\text{mc,th}}$ ) beyond which  $M_{\text{sg}}$  can be as large as the observed value of typical GCs ( $\sim 10^5 M_{\odot}$ ). This  $M_{\text{mc,th}}$  is as large as  $10^7 M_{\odot}$  for a canonical (Salpeter) IMF and it can be smaller for more top-heavy IMFs. The final masses of FG stars can be quite large ( $M_{\text{fg}} \sim 5 \times 10^6 M_{\odot}$ ) in the simulated GCs for  $M_{\text{mc}} = 10^7 M_{\odot}$  and the large fraction of FG stars reside in the halo regions of the proto-GCs. This means that the vast majority of the FG stars need to be lost for the simulated proto-GCs to become genuine GCs dominated by SG stars. This required removal of FG stars has been extensively discussed by previous simulations already.

(4) The two-stage GC formation process (i.e., SG formation after FG formation) through merging of hierarchical SC complexes does not depend strongly on  $M_{\text{mc}}$ ,  $R_{\text{mc}}$ ,  $f_{\text{rot}}$ ,  $D_3$ , and tidal fields of MC-host dwarfs, though the physical properties of simulated GCs depend on these parameters. Threshold gas densities for star formation ( $\rho_{\text{th}}$ ) can significantly influence the final  $M_{\text{sg}}$  such that  $M_{\text{sg}}$  can be lower for higher  $\rho_{\text{th}}$ . If  $\rho_{\text{th}}$  is quite high  $\geq 10^5$ , then SG formation is severely suppressed, which ends up with SCs with small  $M_{\text{sg}}$  that can not be identified as genuine GCs. This result implies that  $\rho_{\text{th}}$  could be similar between FG and SG formation for self-enrichment scenarios to be viable.

(5) Formation of SG stars from AGB ejecta can last as long as  $\sim 10^8$  yr, because gaseous ejecta from AGB stars with different masses thus different main-sequence lifetimes can be accreted onto the proto-GCs. Accordingly, SNe from SG stars formed earlier blow off the accumulated AGB ejecta so that star formation can be severely suppressed. This suppression of star formation ends up with significantly smaller  $M_{\text{sg}}$  in GCs, which implies that the mass budget problem is much more severe than ever thought in the self-enrichment scenario of GC formation with multiple stellar populations. Therefore the formation of GCs with  $M_{\text{sg}} \sim 10^5 M_{\odot}$  requires a very small number fraction of high-mass stars with  $m_s \geq 8 M_{\odot}$  in SG star formation (‘top-light’ IMFs). Such suppression of massive star formation in SG star formation was also pointed out by D10.

(6) The required top-light IMF in SG formation has some important implications both on the observed properties of GCs and young massive SCs and on theoretical studies of star formation. First, even if secondary star formation is ongoing in young massive SCs, massive OB

stars can not be observed in the SCs owing to the lack of such massive stars. This may explain why recent observations of massive young SCs did not detect signs of massive OB stars. Second, the mass budget problem needs to be revisited, given that the mass fraction of low-mass stars ( $m_s \leq 0.9M_\odot$ , i.e., presently ‘alive’ old stellar population) in SG subpopulation can be significantly larger for top-light IMF. Third, a mechanism for suppression of massive stars in dense stellar systems needs to be theoretically understood.

(7) If top-light IMF is not possible in SG star formation, then  $M_{\text{mc,th}}$  can be quite large ( $> 10^7 M_\odot$ ) in any self-enrichment scenario of GC formation owing to very low  $\epsilon_{\text{sf,sg}}$  ( $< 0.1$ ). Therefore the scenario needs to explain how and why such a large  $M_{\text{mc,th}}$  is possible in gas-rich dwarfs (or in other environments) at high redshifts. If the scenario fails to explain the physical origin of such high  $M_{\text{mc,th}}$ , then it would need to be discarded as a viable scenario for GC formation. Thus, a possible IMF variation in star formation within dense stellar systems will need to be investigated in theoretical studies of GC formation based on self-enrichment scenarios.

## 6 ACKNOWLEDGMENT

I (Kenji Bekki; KB) am grateful to the referee for constructive and useful comments that improved this paper. Numerical simulations reported here were carried out on the two GPU clusters, Pleiades and gSTAR kindly made available by International Center for radio astronomy research(ICRAR ) at The University of Western Australia and the Center for Astrophysics and Supercomputing in the Swinburne University, respectively. This research was supported by resources awarded under the Astronomy Australia Ltd’ s ASTAC scheme on Swinburne with support from the Australian government. gSTAR is funded by Swinburne and the Australian Government’s Education Investment Fund. KB appreciate that Amanda Karakas provided stellar yields of AGB stars for this research. KB acknowledges the financial support of the Australian Research Council throughout the course of this work.

## REFERENCES

- Adamo, A., et al., 2012, MNRAS, 426, 1185  
 Ashman, K. M., Zepf, S. E., 2001, AJ, 122, 1888  
 Bastian, N., Gieles, M., Efremov, Y. N., Lamers, H. J. G. L. M., 2005, A&A, 443, 79  
 Bastian, N., de Mink, S. E., 2009, MNRAS, 398, L11  
 Baumgardt, H., Kroupa, P., Parmentier, G., 2008, MNRAS, 384, 1231  
 Bekki, K., 2010, ApJ, 724, L99 (B100)  
 Bekki, K., 2011, MNRAS, 412, 2241 (B11)  
 Bekki, K., 2013, 432, 2298  
 Bekki, K., 2015, MNRAS, 449, 1625,  
 Bekki, K., 2016, submitted to A&A  
 Bekki, K., 2017, MNRAS in press (B17)  
 Bekki, K., Chiba, M., 2007, ApJ, 665, 1164  
 Bekki, K., Freeman, K. C., 2003, MNRAS, 346, L11  
 Bekki, K.; Campbell, S. W.; Lattanzio, J. C.; Norris, J. E., 2007, MNRAS, 377, 335  
 Bekki, K., Tsujimoto, T., 2016, ApJ, 831, 70  
 Bergin, Edwin A.; Tafalla, M., 2008, ARA&A, 2007, 45, 339  
 Blitz, L., Williams, J. P., Invited review for second Crete conference “The Physics of Star Formation and Early Stellar Evolution”, (astro-ph/9903382).  
 Blitz, L., Fukui, Y., Kawamura, A., Leroy, A., Mizuno, N., Rosolowsky, E., 2007, Protostars and Planets V, edited by B. Reipurth, D. Jewitt, and K. Keil, University of Arizona Press, Tucson, p81  
 Carretta, E., Bragaglia, A., Gratton, R. G., Lucatello, S., 2009, A&A, 505, 117 (C09)  
 Carretta, E., et al., 2010, ApJ, 712, L21  
 Dale, J. E., Ngoumou, J., Ercolano, B., Bonnell, I. A., 2014, MNRAS, 442, 694  
 Decressin, T., Meynet, G., Charbonnel, C., Prantzos, N. & Ekström, S. 2007, A&A, 464, 1029  
 D’Ercole, A., Vesperini, E., D’Antona, F., McMillan, S. L. W., & Recchi, S. 2008, MNRAS, 391, 825 (D08)  
 D’Ercole, A., D’Antona, F., Ventura, P., Vesperini, E., McMillan, S. L. W., 2010, MNRAS, 407, 854 (D10)  
 Elmegreen, B. G., 2008, ASP Conference Series, Vol. 388, Edited by Alex de Koter, Linda J. Smith, and Laurens B. F. M. Waters. San Francisco: Astronomical Society of the Pacific, p.249  
 Elmegreen, B. G., Efremov, Y. N., 1997, ApJ, 480, 235  
 Efremov, Y. N., 1995, AJ, 110, 2757  
 Fenner, Y., Campbell, S., Karakas, A. I., Lattanzio, J. C., Gibson, B. K., 2004, MNRAS, 353, 789  
 For, B.Q., Bekki, K., 2017, MNRAS, 468, L11  
 Forbes, J. C., Krumholz, M. R., Goldbaum, N. J., Dekel, A., 2016, Nature, 535, 523  
 Freeman, K. C. 1993, in The globular clusters-galaxy connection, eds. G. H., Smith, and J. P., Brodie, (San Francisco: ASP), ASP Conf. Ser. 48, p608  
 Freeman, K., & Rodgers, A. W., 1975, ApJ, 201, 71  
 Goudfrooij, P., et al., 2014, ApJ, 797, 35  
 Gratton, Raffaele G.; Carretta, Eugenio; Bragaglia, A., 2012, A&ARv, 20, 50  
 Greggio, L., Rensini, A., 2011, Stellar populations. A User Guide from Low to High Redshift  
 Harris, W. E., Pudritz, R. E., 1994, ApJ, 429, 177  
 Hills, J. G., 1980, ApJ, 235  
 Hurley, J. R., Bekki, K., 2008, MNRAS, 389, L61  
 Ikuta, C., Arimoto, N., 2000, A&A, 358, 535  
 Karakas, A. I., 2010, MNRAS, 403, 1413 (K10)  
 Kuzma, P. B., Da Costa, G. S., Mackey, A. D., Roderick, T. A., 2016, MNRAS, 461, 3639  
 Larsen, S. S., Brodie, J. P., Grundahl, F., Strader, J., 2014, ApJ, 797, 15  
 Larson, R. B., 1981, MNRAS, 194, 809  
 Lee, J-W., Lee, J., Kang, Y-W., Lee, Y-W., Han, S-I., Joo, S-J., Rey, S-C., Yong, D., 2009, ApJ, 695, 78  
 Li, C., de Grijs, R., Deng, L., Milone, A. P., 2016, accepted in ApJ (arXiv.161104659)  
 Marshall, J. R., van Loon, J. Th., Matsuura, M., Wood, P. R., Zijlstra, A. A., Whitelock, P. A., 2004, MNRAS, 355, 1348  
 Marino, A. F., Milone, A. P., Piotto, G., Villanova, S., Bedin, L. R., Bellini, A., Renzini, A., 2009, A&A, 505, 1099

Marino, A. F. et al. 2015, MNRAS, 450, 815  
 Milone, A. P., Marino, A. F., D'Antona, F., Bedin, L. R.,  
 Da Costa, G. S., Jerjen, H., Mackey, A. D., 2016, MNRAS,  
 458, 4638  
 Mucciarelli, A., Origlia, L., Ferraro, F. R., Pancino, E.,  
 2009, ApJ, 695, L134  
 Navarro, J. F., Frenk, C. S., White, S. D. M., 1996, ApJ,  
 462, 563 (NFW)  
 Neto, A. F., et al., 2007, MNRAS, 381, 1450  
 Niederhofer, F., et al., 2016, MNRAS in press  
 (arXiv:1612.00400)  
 Phillips, J. P., 1999, A&AS, 134, 241  
 Piotto, G., et al., 2005, 621, 777  
 Rosen A., Bregman J. N., 1995, ApJ, 440, 634.  
 Rosolowsky, E., Engargiola, G., Plambeck, R., Blitz, L.,  
 2003, ApJ, 599, 258  
 Rossi, L. J.; Bekki, K.; Hurley, J. R. 2016, MNRAS, 462,  
 2861  
 Solomon P. M., Sanders D. B., Scoville N. Z. , 1979, in  
 Burton W. B., ed., Proc. IAU Symp. 84, The Large-scale  
 Characteristics of the Galaxy. Reidel, Dordrecht, p. 35  
 Solomon, P. M., Rivolo, A. R., Barrett, J., Yahil, A., 1987,  
 ApJ, 319, 730  
 Spitzer, L. Jr., Hart, M. H., 1971, ApJ, 164, 399  
 Sun, N-C., et al. 2016, ApJ in press (arXiv161106508)  
 Sutherland R. S., Dopita M. A. 1993, ApJS 1993, 88, 2531  
 Thornton, K., Gaudlitz, M., Janka, H.-Th., Steinmetz, M.,  
 1998, ApJ, 500, 95  
 Tsujimoto, T., Nomoto, K., Yoshii, Y., Hashimoto, M.,  
 Yanagida, S., Thielemann, F.-K., 1995, MNRAS, 277, 945  
 (T95)  
 Ventura, P., Di Criscienzo, M., Carini, R., D'Antona, F.,  
 2013, MNRAS, 431, 3642  
 Vesperini, E., McMillan, S. L. W., D'Antona, F., &  
 D'Ercole, A. 2010, ApJ, 718, L112  
 Whitney, B. A., et al. 2008, AJ, 136, 18  
 Wünsch, R., Tenorio-Tagle, G., Palous, J., Silich, S., 2008,  
 ApJ, 683, 683

## APPENDIX A: A WAY TO SET UP INITIAL FRACTAL GASEOUS DISTRIBUTION OF MCS

We generate an initial fractal distribution of gas in a MC as follows. First, gas (SPH) particles with the total particle number of  $N_{\min}$  are distributed within a sphere according to an adopted radial density profile of the MC (i.e.,  $\rho_{\text{mc}}(r) \propto r^{-1}$ ). A random number generator is used in distributing these  $N_{\min}$  particles. This first step is called Level 1 and the initial radius of the sphere is denoted as  $r_1$  for simplicity. Second, at  $i$ th particle's position ( $i = 1, 2, \dots, N_{\min}$ ), new gas particles with the total number of  $N_{\min}$  are distributed within a sphere of  $r_2$  using the same radial profile adopted in Level 1. The radius of the sphere in Level 2 is determined as follows:

$$r_2 = \frac{r_1}{f_{\text{div}}}, \quad (\text{A1})$$

where  $f_{\text{div}}$  is a division factor, which is described as follows:

$$f_{\text{div}} = N_{\min}^{1/D_3}, \quad (\text{A2})$$

where  $D_3$  is the fractal dimension of the MC (as defined

in the main text). Accordingly, the large-scale particle distribution in Level 1 and the small-scale one around  $i$ th gas particle are self-similar. This process is done for each of  $N_{\min}$  particles generated in the Level 1. Thus, the total number of particles used in this Level 2 is  $N_{\min}^{f_{\text{div}}}$ .

If the particle distribution around  $i$ th gas particle in Level 2 is exactly the same as the original particle distribution in Level 1, then the final distribution of gas becomes very artificial ('mathematical') one. In order to avoid this, a random number generator is used each time when gas particle distribution is generated for a given (adopted) radial distribution of gas. By doing so, the final distribution of particles become more natural in the present study. This process of generating a self-similar particle distribution is repeated in Level 3, 4, 5 etc until the total number of particles becomes the adopted number of particles of a MC in a simulation (i.e.,  $N_g \sim 10^6$ ). In the present study  $N_{\min}$  is set to be 32, which ensures that the initial distribution of gas particles in Level 1 can be a proper representation of the adopted radial profile. If  $N_{\min}$  is too small, then the initial distribution is not so similar to the adopted profile. On the other hand,  $N_{\min}$  is large (e.g., 100), then the number of division becomes smaller. We consider that the above number of 32 is appropriate for the present investigation of GC formation within fractal MCs.

In order to give random motion of gas particles within a fractal MC, we adopt the following model. We here consider that the total number of sub-groups of gas particle at the final Level of division (for the fractal mass distribution of a MC) is  $n_{\text{gr}}$ . These sub-groups have random motion within the MC characterized by velocity dispersion  $\sigma$ . Accordingly,  $\sigma$  is determined as follows:

$$T_{\text{ran}} = \frac{1}{2} \sum_{k=1}^{n_{\text{gr}}} M_{\text{gr},k} \sigma^2, \quad (\text{A3})$$

where  $T_{\text{ran}}$  is the total random (kinetic) energy of the MC and  $M_{\text{gr},k}$  is the mass of each sub-group. Using a random number generator and assuming an isotropic velocity dispersion, the 3D velocity of each sub-group is given for the derived  $\sigma$ . In some models, a MC has initial rigid rotation with the amplitude of  $\Omega$  (constant). Each sub-group's  $\Omega$  is therefore determined as follows:

$$T_{\text{rot}} = \frac{1}{2} \sum_{k=1}^{n_{\text{gr}}} R_k^2 M_{\text{gr},k} \Omega, \quad (\text{A4})$$

where  $T_{\text{rot}}$  is the total rotational energy of the MC and  $R_k$  is the projected distance of  $k$ th sub-group from the MC's center. Using the derived  $\Omega$  and  $R_k$ , rotational velocities of gas particles within each sub-group are calculated. Gas particles within a sub-group are assumed to have the same velocities in the present study.